THE EFFECTS OF LAND SUBSIDENCE ON SEDIMENT TRANSPORT AND CHANNEL BED RESPONSE IN THE SAN JOAQUIN VALLEY

DRAFT Plan B Technical Report

Prepared by:

Susan Cundiff, P.E., CFM

Department of Civil and Environmental Engineering

Colorado State University

In partial fulfillment of the

M.S. Plan B Degree Requirements

Adviser: Dr. Pierre Julien

Spring 2019

Susan Cundiff, P.E., CFM

1. Contents

Susan Cundiff, P.E., CFM

2. Table of Figures

Abstract

This study examines how land subsidence affects sediment transport in an alluvial channel. The San Joaquin River, located in the Central Valley of California, has been subjected to considerable groundwater pumping to support irrigated agriculture. The mining of the groundwater has induced severe subsidence, which has implications on the sediment transport both within the San Joaquin river and its Eastside Bypass. The Eastside Bypass is the focus of this study because subsidence rates ranged from 0.174 to 0.716 feet/year, with the maximum subsidence rate in its central reach.

A conceptual model was used with simple geometry to obtain qualitative results. Sediment transport calculations were carried out with the Engelund-Hansen formula. When the slope increased from 19 to 25 cm/km at 10 m^2/s, the conceptual model predicted a sediment transport rate increase from 130 to 161 metric tons/m.day. An increase in sediment transport is observed in the upper reach with steeper channel slopes while sediment accumulates in the flatter lower reach.

The model HEC-RAS 5.0.5 with mobile boundary capabilities was applied to obtain more detailed results. The HEC-RAS model covered 41 miles of the Eastside Bypass with the 2016 channel geometry discretized in 575 cross sections based on detailed Lidar data reduced to 100 points per cross-section. The model simulated a 13-year period representative of relatively wet hydrological conditions. Quantitative HEC-RAS model results with subsidence show almost 2 feet of degradation on the upstream side of the subsidence induced sag. In the downstream portion where slope decreased, the model predicted about 2.9 feet of aggradation due to subsidence. Over the 13-year simulation period, the difference in sediment mass accumulation reached approximately 31,700 tons between the model simulations with/without subsidence.

Susan Cundiff, P.E., CFM

1. Introduction

This paper studies the effects of subsidence on sediment transport in the Bypass System of the San Joaquin River. The San Joaquin River drains the southern portion of the Central Valley of California (**Figure 1**). Development in this region was made possible with over a century of water development (McBain & Thrush, Inc. (eds.), 2002). Water development for this region includes a vast network of canals, bypasses and reservoirs. In addition to surface water development, additional water demands are met through groundwater pumping (McBain & Thrush, Inc. (eds.), 2002). Groundwater pumping has led to reduced aquifers levels and major land subsidence, or lowering of the land surface (Poland, 1984; Bull & Miller, 1975). The alterations made to the San Joaquin River to support development of the region have changed the river ecosystem and caused a general reduction in wildlife populations and their movement (McBain & Thrush, Inc. (eds.), 2002). In 1988, a coalition of environmental groups led by the Natural Resources Defense Council filed a lawsuit against the U.S. Bureau of Reclamation (Reclamation) and a Settlement Agreement was reached in 2006 (McBain & Thrush, Inc. (eds.), 2002). The Settlement Agreement requires restoration of natural ecological functions in a manner that does not adversely impact the water users. Water managers must meet both of these requirements of the San Joaquin River Restoration Program (Program) as defined by the Settlement Agreement.
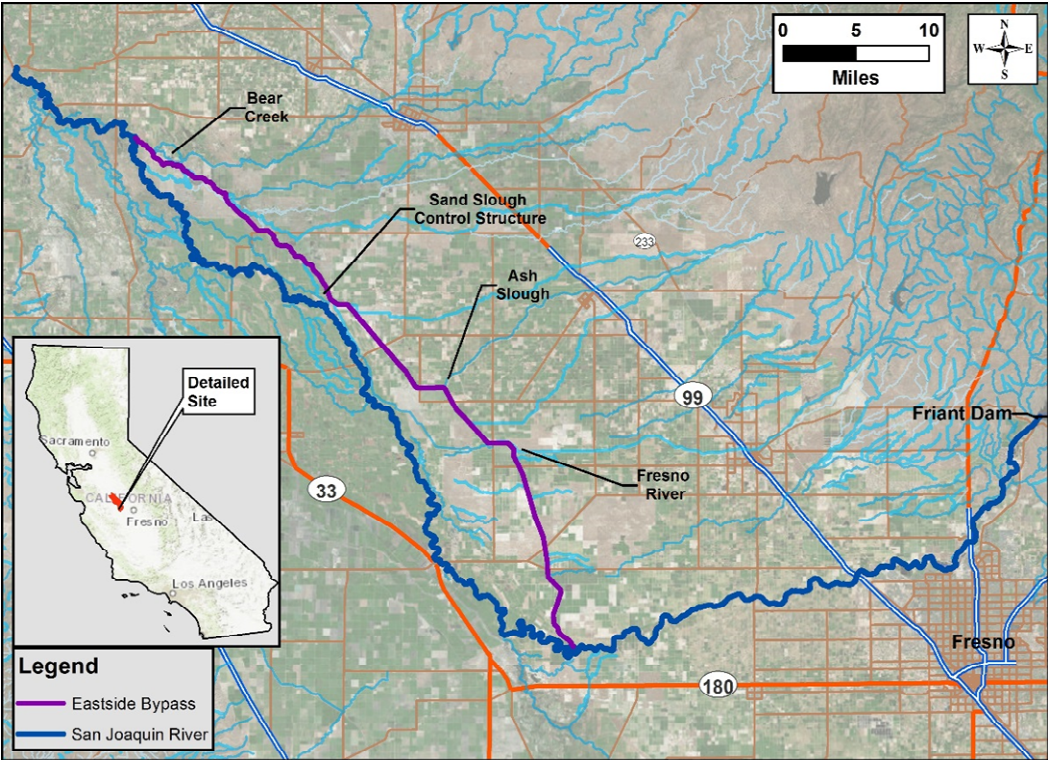
Figure 1   Site map of San Joaquin River and Bypass System.

Susan Cundiff, P.E., CFM

Water managers have had to anticipate the effects on the river and Bypass System because of the changes that are taking place as a part of the Program. One component of the restoration program is designing new and old structures to be suitable for fish passage and subsidence adds challenges to the design and operation of water delivery. Subsidence causes channel capacity to be reduced (Swanson, 1998) and also changes the location and magnitude of sedimentation issues. Water managers actively maintain channel capacity in the Bypass System by physically removing sediment (Tetra Tech, 2015a). Being able to anticipate how subsidence will change the way in which sediment is transported is an asset to water managers in the SJR valley.

One tool that can be used to anticipate future water-surface elevations and sedimentation issues is HEC-RAS (Hydrologic Engineering Center-River Analysis System) (USACE, 2018). HEC RAS 5.0.5 (USACE, 2018) has the capability to model sediment transport with a mobile boundary in conjunction with subsidence. This software can be used to determine how subsidence will change sediment transport rates and identify areas of concern for meeting water delivery demands.

Areas of erosion and deposition are occurring in the Bypass System. Subsidence is likely exacerbating these processes, causing areas of erosion and deposition that can further reduce in-channel capacity. HEC-RAS's mobile boundary sediment transport functionality is a valuable tool to assess how flow changes and subsidence work together to change sediment transport (USACE, 2018). Development of mobile boundary sediment transport models can be labor intensive and require significant resources. HEC-RAS has the capability to apply incremental subsidence to mobile boundary simulations to help water managers identify areas of erosion and deposition that are caused by and/or exacerbated by subsidence. This paper identifies how incorporating subsidence into the sediment transport model affect the results. This will be accomplished by answering the following questions using HEC-RAS 5.0.5:

a) How does subsidence change the amount of sediment transported?
b) How does HEC-RAS quantify the changes to sediment transport caused by subsidence?

2. Literature Review

The tool used in this paper is HEC-RAS 5.0.5 (USACE, 2018) , which has the capability to model sediment transport with a mobile boundary in conjunction with subsidence. The subsidence feature was first added to HEC-RAS 5.0, and has remained available to later versions (Dahl et al.,2018). This software can be used to determine how subsidence will change sediment transport

Susan Cundiff, P.E., CFM

rates and to identify areas of concern for meeting water delivery demands. The precursor to the mobile boundary capability in HEC-RAS was HEC-6 (USACE, 1993).

The mobile boundary component of HEC-RAS offers many equations for estimating sediment transport. For consistency with previous studies conducted on the San Joaquin River by the U.S. Bureau of Reclamation and others, (Huang & Greimann, 2008; MEI, 2002; Tetra Tech, 2010; Tetra Tech, 2015a) the Engelund-Hansen equation was selected again for this analysis. Bed material sampling for some of these studies characterized the sediment in the system as primarily silt and sand with typical sizes ranging from 0.02 -mm to 0.5 -mm (Tetra Tech, 2015a). The Engelund Hansen equation is an equation that estimates the "Total Load" of alluvial beds (Engelund & Hansen, 1967). Because the Engelund-Hansen equation is a total load equation, it does not assume any portioning of size class, nor separating the transported load into wash load or bed load. Appropriate size class fractions for this equation are 0.19 mm-0.93 mm (USACE, 1998), which is consistent with the Bypass and the SJR in the study reach. The equation is a combination of the dimensionless ϕ, θ and f, the friction factor; thus, the equation is not specific to SI (Standard International) or Imperial units.

Engelund-Hansen Equation: $\mathbf{g_s = 0.05 \gamma s\, V^2 \sqrt{\dfrac{d_{50}}{g\left(\frac{\gamma s}{\gamma}-1\right)} \left(\dfrac{\tau_0}{(\gamma_s-\gamma)d_{50}}\right)^{\frac{3}{2}}}}$

Where: g_s=Unit sediment transport

γ= Unit weight of water

γ_s= Unit weight of water

V=Average channel velocity

τ_0=Bed level shear stress

d_{50}= Median Particle size

Changes to average channel velocity and bed level shear stress will have the greatest effect to the unit sediment transport as these terms are in the numerator and squared and raised to the 1.5 power, respectively. Channel responses to perturbations to a system, such as land subsidence, will change the shear stresses and velocities by changing the bed slope. Changes to slope, embedded in the shear stress term, will change the unit sediment transport rates.

The incremental subsidence is the unique component of the HEC-RAS mobile boundary function. The definition of subsidence is helpful in understanding why one would be interested in how

Susan Cundiff, P.E., CFM

subsidence affects sediment transport. Land subsidence is the sinking or lowering of the ground surface (Poland, 1984). According to H.B. 1041, 106-7-103(10), the subsidence is legally defined as follows: is:

 "Ground subsidence" means a process characterized by downward displacement of surface material caused by natural phenomena such as removal of underground fluids, natural consolidation, or dissolution of underground minerals, or by man-made phenomena such as underground mining.

As suggested by the legal definition, there are several potential causes of land subsidence. The two primary mechanisms through which subsidence can are occur are mechanical or chemical alteration of the underlying materials that support the ground surface (Allen, 1969; Galloway et al., 1999). Mechanical mechanisms of subsidence are the withdrawal of underground fluids, both groundwater, and fluids from oil and gas extraction, and the collapse of the ground because of removal of underlying support such as in subsurface mining. Subsurface salts and gypsum can go into solution and remove support for the surface which can result in collapse of the ground surface (MEI, 1996). The creation of underground pathways which can transport sediment particles, also known as piping, can also remove support for the surface. Lateral subsurface flow of plastic materials such as salts, shales and clays can occur when loading changes, and causing subsidence (Allen, 1969). Subsurface sediments can become compacted when loads on the surface increase, the interstices are drained, vibration occurs, or when they become wet (hydrocompaction). Two additional geologic processes that can cause subsidence are tectonic movements and volcanic activity (Allen, 1969).

Groundwater withdrawal is the primary cause of subsidence in the Central Valley of California (Poland, 1984). According to Poland (1984) three main types of groundwater withdrawal contribute to land subsidence: oil, gas, and water associated with extraction of natural resources, removal of hot water or steam for power generation, and groundwater withdrawal. While the Central Valley is susceptible to subsidence due to tectonic movements (Ouchi, 1985), the extraction of groundwater has caused the most drastic subsidence. Groundwater withdrawal in the Central Valley has caused the unconsolidated alluvial and lacustrine deposits (Poland, 1984) to consolidate and subsequently subside. In addition to ground water pumping which causes subsidence to occur at much deeper depths (Poland, 1984; Lofgren, 1960) notes that near surface subsidence occurs when the soils are wetted through irrigation of fields and water flowing in canals.

Due to the implications of subsidence federal and state agencies have been monitoring subsidence in the San Joaquin Valley since the early 20th century. Subsidence occurred at rapid rates in the 1950s and 1960s (Swanson, 1998). Between 1926 and 1969, subsidence in the San Joaquin Valley exceeded 28 feet (Poland, 1984) (**Figure 2**). Subsidence rates decreased in the

Figure 2   From the UNESCO Guidebook, Land Subsidence "Joseph F. Poland of U.S. Geological Survey stands near bench mark S661 southwest of Mendota in the San Joaquin Valley, California. The bench mark site subsided 9m from 1925 to 1977, because of intensive withdrawal of ground water. Signs on the power pole indicate the respective positions of the land surface in 1925, 1955, and 1977." (Poland, 1984)

mid-1970s when surface-water deliveries were readily available and periods of drought were typically the only times when increased ground-water pumping was necessary (Swanson, 1998). Subsidence rates began to increase again starting in the mid-1990s as surface water was designated for environment uses including but not limited to salmon and similar species, tighter regulations on salinity in the delta region and water fowl (Swanson, 1998).

Subsidence often presents as a bowl shape over larger regions with the lowest portion of the bowl at the epicenter of the pumping (Farr et al., 2015). This bowl shape creates a sag in channel profiles which increase the channel slopes on the uphill side of the sag thus increasing velocities and erosion of unlined channels and on the downstream side of the sag, which can reduce channel capacity (Swanson, 1998). Sedimentation in the channel could further reduce channel capacity. Increased slope and potentially increased sediment transport rates could cause channel incision which can create a positive feedback cycle of increased stream power and upstream incision and channel bank degradation (Brookes, 1988).

Channel response to subsidence depends on which side of the subsidence axis one is studying (Ouchi, 1985; Schumm et al., 2000). Lateral subsidence has been shown to cause lateral channel migration (Straub et al., 2013). Sediment can be captured in subsidence zones (Ouchi, 1985; Schumm et al., 2000) and cause degradation in the downstream direction because of a lack of sediment supply. Begin et al., (1981) demonstrated with flume studies that channel degradation rates are attenuated exponentially in the upstream direction from the disturbance area. If a channel is unconfined, it will migrate laterally and increase sinuosity to account for changes in slope due to subsidence (Ouchi, 1985; Schumm et al., 2000). However, confined channels, such as the Bypass System will generally degrade.

The amounts and rates of subsidence in the San Joaquin Valley are astonishing. In 1970 as much as 28 feet of subsidence had occurred in the San Joaquin Valley with over half of the region having subsided by 1 foot or more (Poland, 1984). Current rates of subsidence in the San Joaquin Valley are nearly 1 foot per year (SJRRP, 2015). Concrete linings of canals have experienced damage as a result of large amounts of land subsidence. Subsidence values of up to 10 inches from May 2014 to January 2015 have been measured with interferometric synthetic-aperture radar (InSAR) (Farr et al., 2015) in an area along the Bypass System.

3. Site Description

The portions of the Eastside Bypass (Bypass) System, constructed in the late 1960s (DWR, 1969), that were modeled for this study flow from the Chowchilla Bifurcation Structure near Mendota, CA to the lower end of the Middle Eastside Bypass where the Mariposa Bypass can deliver flows into the San Joaquin River. The Eastside Bypass was constructed parallel to the San Joaquin River and was generally constructed as a trapezoidal channel with levees built from the spoils with the main purpose of water conveyance (DWR, 1969). Tributaries to the Eastside Bypass include Ash Slough, Berenda Slough, and flows from the San Joaquin River's Reach 4A through the Sand Slough Connector Channel (**Figure 3**).

The Bypass System is 41 miles long and has an overall slope of 0.00033 feet/feet. Alluvial sands and soils into which the Bypass Channel was constructed generally consist of native and non-native soils (Tetra Tech, 2015a). Many of the soils are cohesive in the upper end of the Chowchilla Bypass. For the purposes of this study cohesive soils were removed from the sediment transport model. Median soil grain sizes in the model range from 0.02-mm to 0.5-mm.

Susan Cundiff, P.E., CFM

Figure 3   Modeled Reaches along the Bypass system of
the San Joaquin River.

4. Methodology

A mobile boundary model is a hydrodynamic model that takes into account the hydraulics and hydrology of a river system and adjusts the bed geometry based on the sediment transport of those parameters. A mobile boundary sediment transport model was used to understand how subsidence impacts the sediment-transport on the Bypass system. A conceptual mobile boundary model was developed by Cundiff (2017) in the River Mechanics course at Colorado State University. This model is set up on a unit discharge basis and looks at how the bed will change and respond when sediment is transported. A second conceptual mobile boundary model that

was used was a version that had subsidence applied to it. This allowed the slopes to change within the study reach and to view the resulting sediment transport capacity. Lastly, a more sophisticated mobile boundary model, the sediment-transport functionality of HEC-RAS 5.0.5 (USACE, 2018) was used. The sophisticated mobile boundary model was developed to do three simulations; a first version with no subsidence to act as the control will be referred to as No Subsidence, a second version that simulates the incremental subsidence, referred to as Subsidence, and a final version that starts and the final, fully subsided elevations referred to as 2029. The following sections describe the development of these mobile boundary models.

4.1   Conceptual Mobile Bed Model Methodology

The three components to understanding how the features in a river change are: flow or hydraulics, sediment transport, and bed evolution. A fixed bed step-backwater model illustrates the effects of slope changes and unit discharge changes on the hydraulics of a river. The application of the simple mobile bed model will demonstrate how changes to the slope changes the magnitudes of the sediment transport capacities. To be consistent with sediment transport modeling on the San Joaquin River and Bypass System, the Engelund-Hansen equation was used in this model (MEI, 2002; Huang & Greimann, 2008; Julien, 2010).   The model was executed for one hundred days.

The mobile bed model is 45,000 meters long, composed of 131 cross sections in three reaches and is assumed to be a wide-rectangular channel where hydraulic radius and depth, h, are assumed to be equal (Cundiff, 2017). In this model the slopes of the reaches have been altered from the original version to S_1=0.0004 m/m, S_2=0.0008 m/m, and S_3=0.0002 m/m for Reaches 1, 2, and 3, respectively. For this exercise channel widths remain constant. The model was executed for 100 days with results written at 1 day, 10 days, 50 days and 100 days.

A second version, the subsided conceptual model of the simple mobile boundary model was executed for 100 days. This version of the model had the initial bed lowered and slopes adjusted to simulate subsidence. The subsidence was varied spatially such that the resulting initial slopes for this version are S_1=0.0003 m/m, S_2=0.0008 m/m, and S_3=0.0003 m/m for Reaches 1, 2, and 3, respectively.

4.2   HEC-RAS Mobile Bed Model Methodology

This HEC-RAS model was originally developed in HEC-RAS 5.0.3 (USACE, 2016) to study the effects of subsidence and sediment transport on channel capacity for the Department of Water Resources in support of the San Joaquin River Restoration Program (DWR, 2018; Tetra Tech, 2015b; Tetra Tech, 2015c). This paper is only concerned with sediment transport rates, volumes

and the bed changes associated with subsidence using HEC-RAS 5.0.5 (USACE, 2018). However, the framework of the model geometry and supporting data were established for prior efforts conducted by Tetra Tech (Tetra Tech, 2015b).

4.2.1 Geometry Development

The modeled extents for this exercise include the Chowchilla Bypass, Upper and Middle Eastside Bypasses, and Reach 4A. Models for each of these river and Bypass segments were initially developed based on 2008 LiDAR elevations, but the geometry in the models were subsequently updated to reflect October 2013 elevations based on levee profile surveys (Tetra Tech, 2015d) because significant subsidence had occurred in that 5 year time frame. The various model segments were combined to form a single network model, to provide downstream boundary conditions, that is water surface elevations, and sediment supply from upstream reaches that are dependent on the immediate condition during the simulation. The model contains 41 miles of Eastside Bypass cross sections, 13 miles of Reach 4A cross sections for a total of 575 cross sections in the model. Reach lengths are on average, 500 feet.

To improve the computations of the model a few techniques were used to simplify the model geometry. Geometry station and elevation points for each cross section were filtered with the "Cross Section Points Filter" tool in HEC-RAS. Points were filtered to approximately 100 per cross section. "Lids" on structures, blocked obstructions and ineffective flow areas were removed in the geometry. Adjustments to the cross section geometry were made to remove low points previously removed from conveyance by ineffective flow areas as ineffective flow areas are not subsided in the simulations (**Figure 4**). "Internal Bridge XS" do not subside during the mobile boundary simulation and so these were removed from the model as well. Cross sections spaced closely together were removed to improve the consistency of cross section spacing. It is important to have consistent cross section spacing to allow for uniform settling of sediment (Julien, 2010). Inconsistent spacing of cross sections, or inconsistent control volumes, will result in unrealistic deposition or erosion.

4.2.2 Subsidence Development

The geometry in the models was based on the October 2013 timeframe. Because the hydrologic simulations (described in more detail below) start on March 1, 2016, the model geometry was adjusted to represent the March 2016 elevations. Subsidence in the San Joaquin Valley is happening at rapid rates and it is important to accurately represent the elevations as closely as possible. The adjustment was made by first determining how much subsidence had occurred from

Susan Cundiff, P.E., CFM

the October 2013 to December 2015 period, which was the date of the most recent subsidence surveys at the time of development. Reclamation collects subsidence elevation information every six months to monitor the subsidence (SJRRP, 2014). Once the amount of subsidence from the October 2013 to December 2015 period was determined, the model elevations were adjusted to the March 2016 time frame by using the rate determined from the total amount of subsidence from October 2013 to December 2015.

An annual subsidence rate was applied to the 13-year simulation to account for future subsidence. This rate was determined from the Reclamation subsidence data and was assumed to continue into the 13-year period at the same rate as the recent past (2011 to 2015) (**Figure 5**). A constant and unique rate was applied to each cross section for the entire 13-year simulation; however, these rates varied spatially. Spatial variation in subsidence rates along the Bypass profile ranged from 0.174 to 0.716 feet/year. **Figure 6** shows the total subsidence estimated for the 13-year simulation.

Susan Cundiff, P.E., CFM
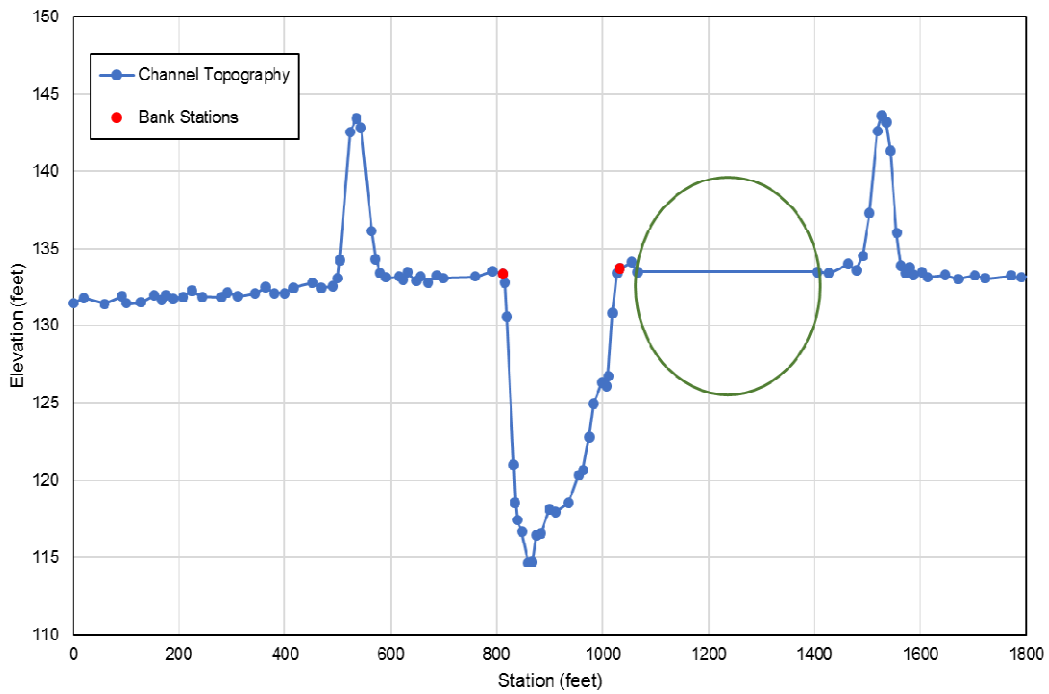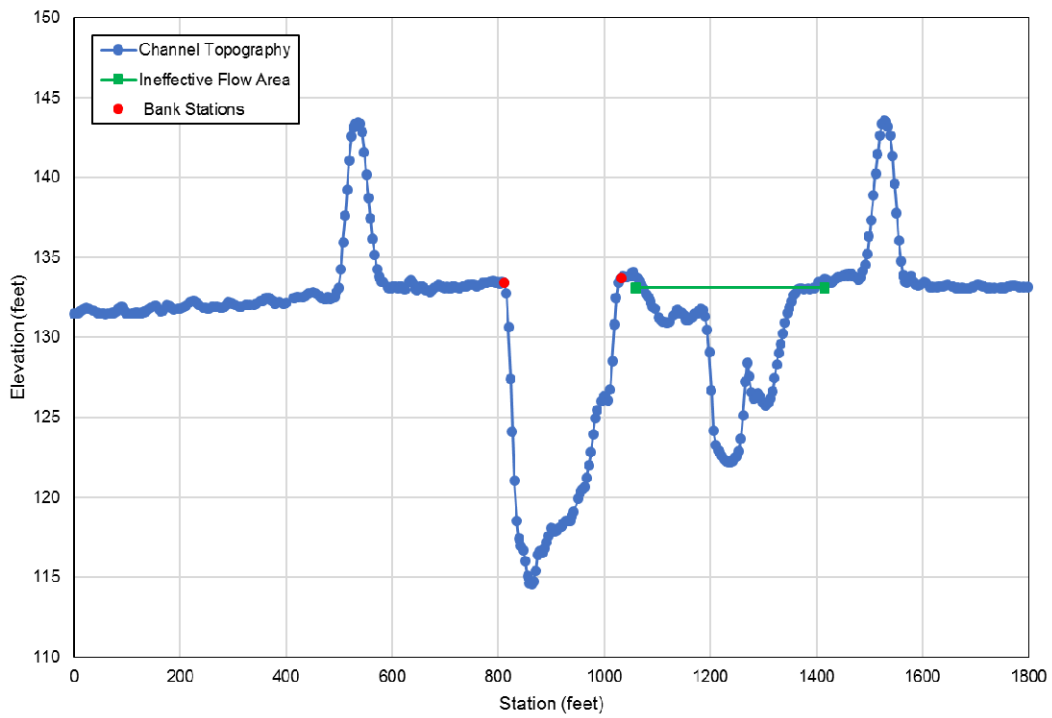
Figure 4   Example cross section demonstrating the filtering of station-elevation points and the adjustment to account for ineffective flow areas.

Susan Cundiff, P.E., CFM
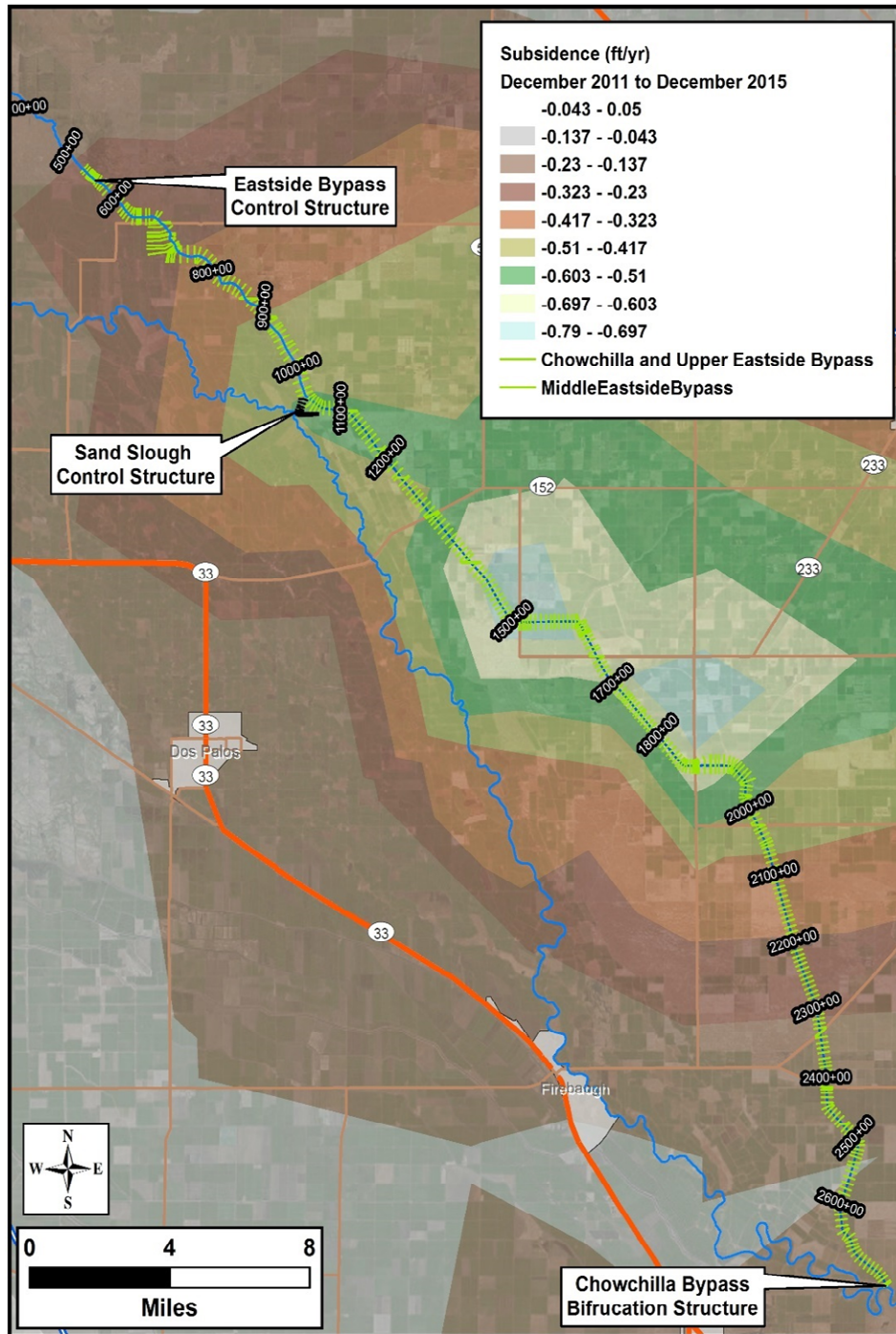
Figure 5   The subsidence rate from 2011 to 2015 that was used to determine the total amount of subsidence in the 13-year simulation. Data collected by Reclamation.

Susan Cundiff, P.E., CFM
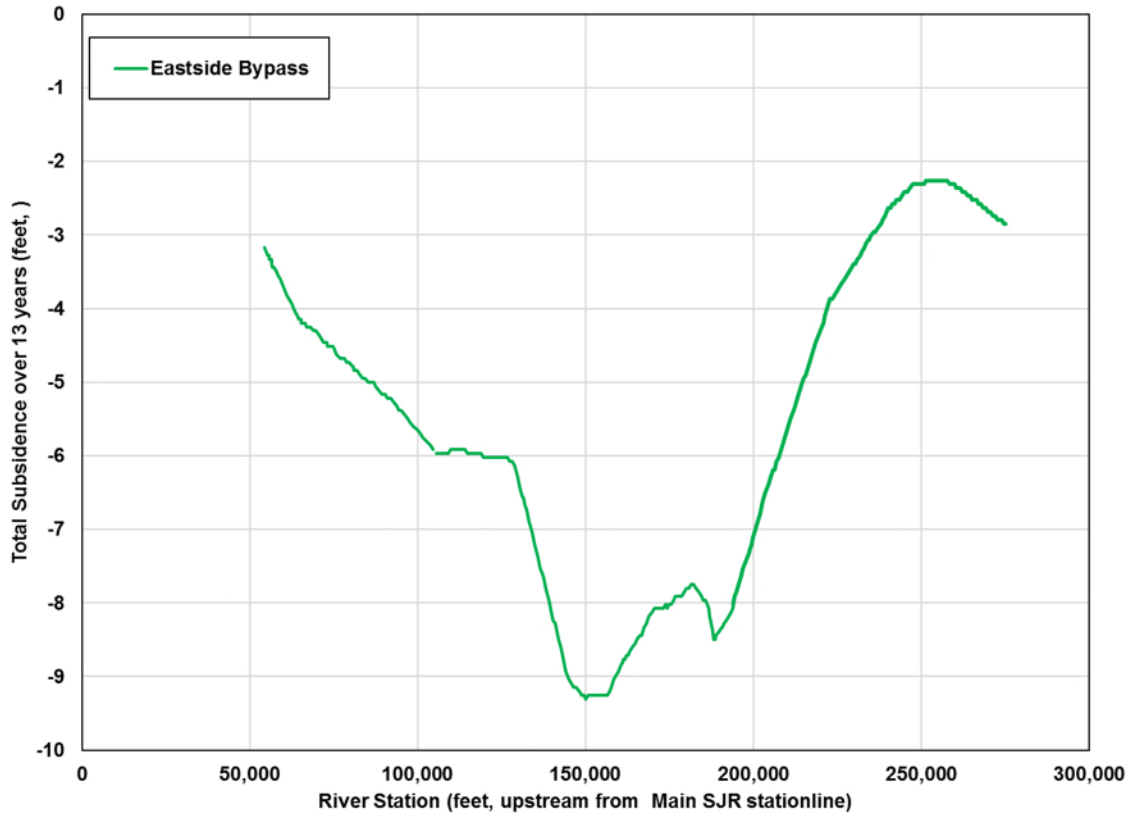
Figure 6   Total Subsidence applied to the model over the 13-year simulation.

The average channel slope in the MESB is 0.00021 feet/feet, UESB is 0.0006 feet/feet, and slope in the Chowchilla Bypass is 0.0002 feet/feet, and the Reach 4A the average channel slope is 0.0002 feet/feet at the beginning of the 13-year simulation. After the 13-year simulation, subsidence has reduced the average channel slope in the MESB to 0.00020 feet/feet and 0.0005 feet/feet in the UESB, while the slope increases in the Chowchilla Bypass to 0.0003 feet/feet and the average channel slope in Reach 4A is 0.0003 feet/feet.

4.2.3   Sediment Transport Methodology Development

The sediment transport methodology used in this HEC-RAS model is based on the mobile bed sediment-transport model developed in HEC-6T by Tetra Tech in 2014 (Tetra Tech, 2015b). This version of the model was developed by using the model geometry (cross-sectional geometry, bank stations, reach lengths, hydraulic roughness and coefficients of expansion and contraction) from the source HEC-RAS models described above. Sediment data used in the HEC-6T model were coded into the HEC-RAS model used in this exercise as well as including the gradation of

the resident bed material [bed sediment reservoir (BSR)]. Unlike the HEC-6Tmodel the depth of the of the BSR and the cohesive sediment erosion/deposition parameters were changed. The rating curves defining the load and gradation of upstream and tributary loads by discharge are consistent to the earlier modeling efforts completed by Tetra Tech.

Computational controls for the sediment-transport function were imported from the HEC-6T model (Tetra Tech, 2015b) and specify the use of the Engelund-Hansen sediment-transport equation. The hydrologic data (i.e. flow records or flow series) were based on the Riverware data described below. Computation intervals specific to the flow series were imported from the HEC-6T modeling (Tetra Tech, 2015b). Flow series were included for the upstream end of the Chowchilla Bypass, Reach 4A and the two tributaries on the Bypass, the Fresno River and the Ash Slough. Sediment inflows from these tributaries are accounted for as rating curves. These rating curves were developed for the HEC-6T model (Tetra Tech, 2015b).

These rating curves may slightly overestimate the amount of sediment transported into the Bypass for a given discharge because the available hydraulic models used to develop the rating curves did not account for backwater conditions in the Bypass. Additional required model input that was imported from the HEC-6T model include hydraulic weighting parameters; the number of bed exchange iterations per time step; specification of the average energy slope for use in the sediment-transport equation; and the method for computing the steady-state friction slope.

4.2.4 Sediment Development

In 2013, Tetra Tech collected samples along the Chowchilla and Eastside Bypasses (Tetra Tech, 2015b) and these samples were used to develop the characteristic gradations used in the HEC-RAS model (**Figure 7**). The sediment gradations used to characterize Reach 4A were developed from samples collected by Reclamation (SJRRP, 2008). The upstream boundary condition selected for the Chowchilla Bypass and Reach 4A is the equilibrium load method as this method calculates an equilibrium sediment-transport capacity at each time step. This method introduces the sediment loads into the next downstream cross section as a time series. Two lateral inflows were used to represent the contributions from the tributaries, Fresno River and Ash Slough. There were sediment data available for these two tributaries so the nearest sediment gradation from the Bypass was used in SamWin (USACE, 2003) with hydraulics from the Central Valley Floodplain Evaluation and Delineation program (CVFED) models (RBF, 2013).
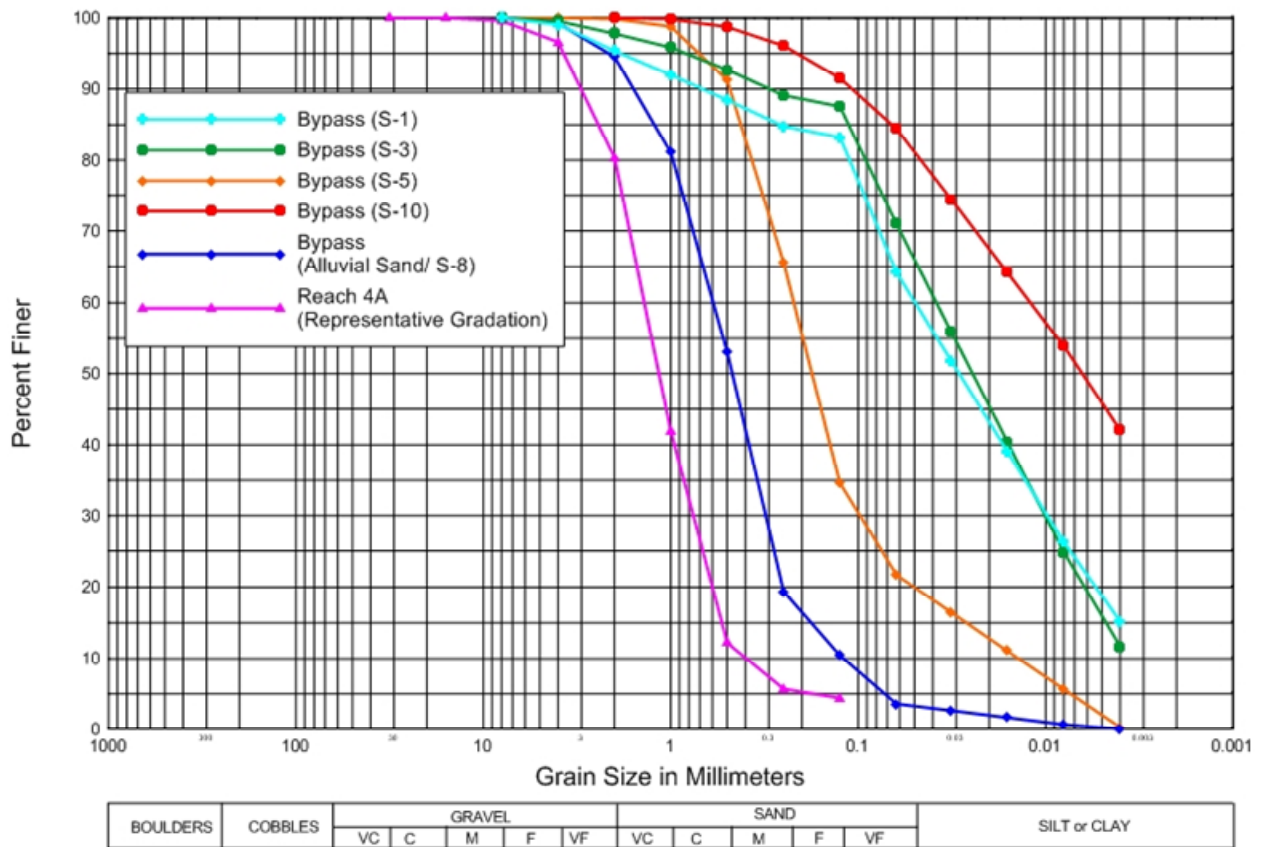
Figure 7   Sediment gradations used in the models from DWR, 2018:"Figure 7. Bed-material sediment sample gradations used in the HEC-RAS mobile boundary model to represent the sediment along the Bypasses and Reach 4A. Note: Bypass sample numbers denoted by (S-#)."

4.2.5   Hydrology Development

The hydrograph used in the 13-year simulation is from a portion of the 83-year Riverware® simulation of the SJR and Bypass System that completed by Reclamation (Reclamation, 2012). The simulated hydrographs are from Water Year 1922 (WY1922) to WY 2003 and were conducted to evaluate several scenarios for Restoration operating rules. The hydrologic simulations represented flow operations without Restoration Flows, also known as Existing Flows. The main difference between these operating rules in how flow is released from Friant Dam and where flows are diverted at the Chowchilla Bifurcation Structure. Under existing conditions most of the flow is diverted into the Chowchilla Bypass. The annual flow volumes released from Friant Dam are larger under the restoration flows even though peak flow events are larger under the existing conditions. For the purposes of this study the Existing routing was selected to have greater volumes of water and therefore sediment transport within the Bypass study reach.

23   Susan Cundiff, P.E., CFM

Because the simulation is only 13-years long and in order to have higher rates of sediment transport, the wettest 13-year period was selected for the sediment transport modeling (DWR, 2018) (**Figure 8**). The hydrograph for the 13-year simulation for various locations along the Bypass system are shown in **Figure 9**. The downstream end of the Bypass system has two peak events in excess of 12,000 cfs in the 13-year simulation. There are six flood periods that have peaks in excess of 4,000 cfs. **Figure 10** shows flow duration curves of the discharges in the
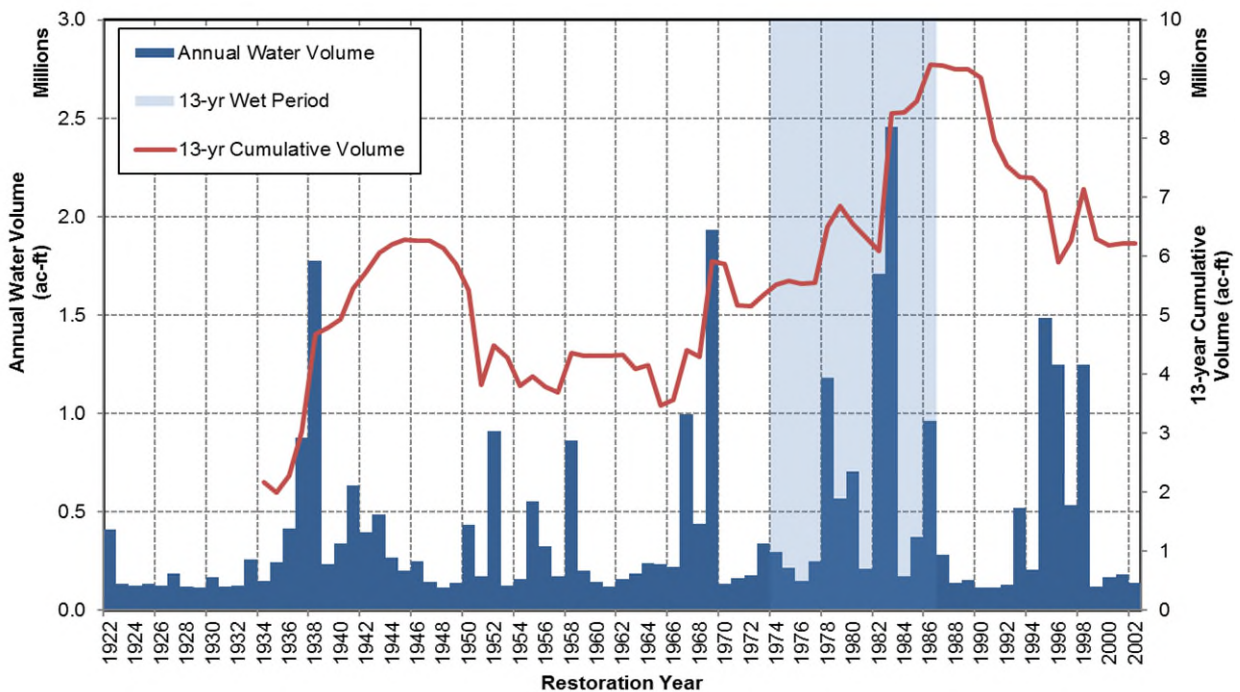
Figure 8   Annual water volume and cumulative volume for 13-year periods during the 83-year simulation. The light blue section highlights the 13-year period with the highest cumulative volume of water in the system.

system at various locations. In the upstream end of the reach it shows that the Bypass System only has flows greater than 100 cfs about 20% of the time. This portion of the channel only receives flood flows from the Mainstem of the San Joaquin River (SJR). The Fresno River and Ash Slough contribute significant flows with locations downstream of those tributaries, Sta 1488+06.4, having discharges of greater than 3 cfs at least 78% of the time. Flow contributions from Reach 4A and the Mainstem of the SJR exceed 4 cfs about 79% of the time.
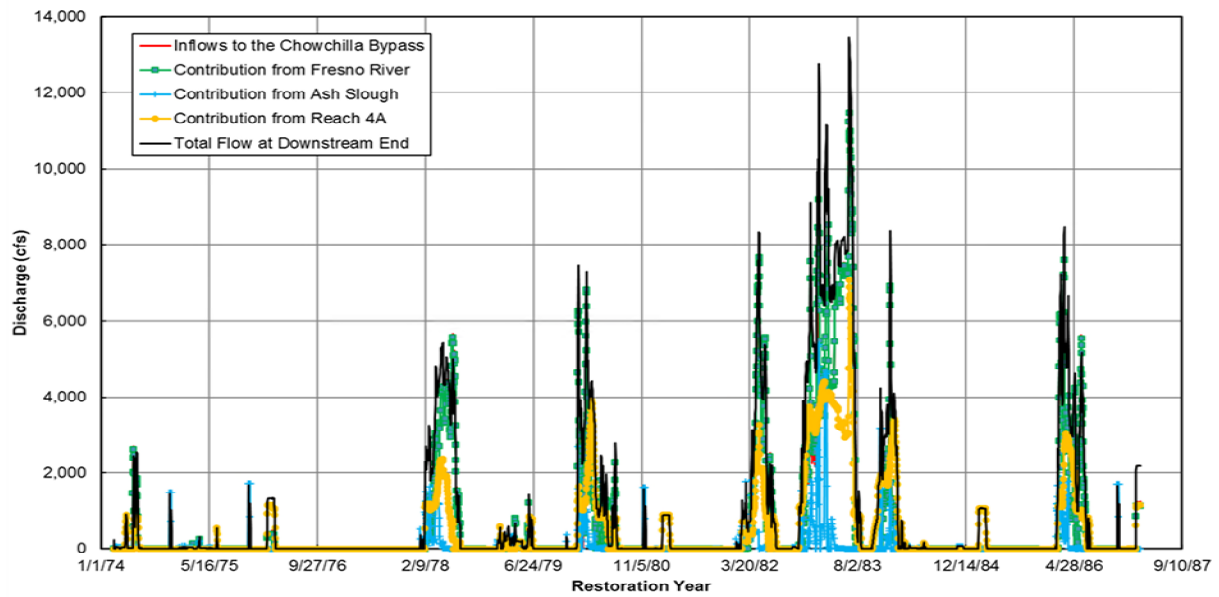
Figure 9   Hydrograph of the 13-year run at various points along the Bypass System.
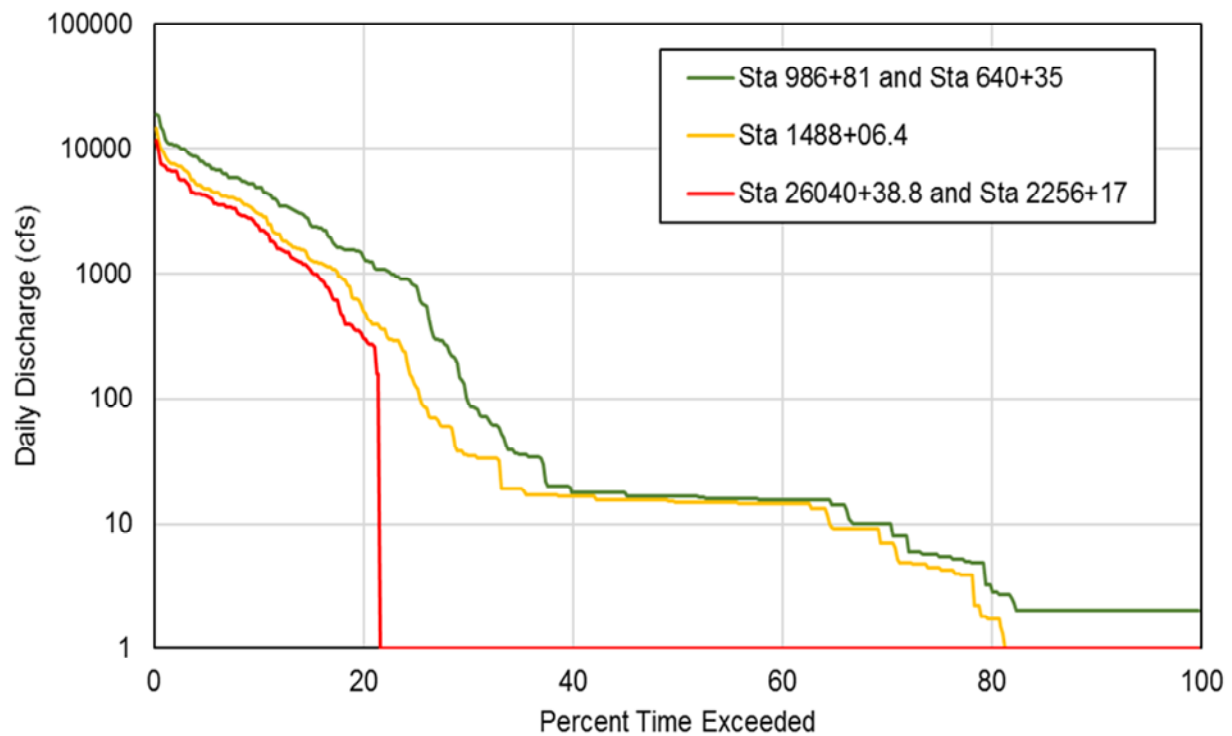
Figure 10   Flow duration curve of the hydrographs in the Bypass System during the 13-year simulation.

Susan Cundiff, P.E., CFM

5. Results

5.1 Results of Conceptual Model

The conceptual model was executed for three different unit discharges; 1 cms/m, 5 cms/m and 10 cms/m. A simulation time of 100 days was chosen (Cundiff, 2017) and bed elevations, water-surface elevations and sediment transport rates recorded at Day 1, Day 10, Day 50 and Day 100. **Figure 11** shows the channel bed and water-surface elevation for the 100 day duration for the 1cms/m simulation. The beginning bed and water-surface profiles show much more distinct breaks of slope than the Day 100 profiles as bed profile morphs through time with sediment transport. **Figure 12** shows the sediment transport rate for the duration of the simulation for the 1 cms/m run. The sediment transport rates for Day 1 are generally higher in Reach 2 and lower in Reaches 1 and 3 because Reach 2 has higher channel slopes and therefore higher velocities than the bounding reaches. Because 1 cms/m is a low unit discharge this channel moves sediment at rates less than 16 metric tons per day. As time progresses the sediment transport rates in Reach 2 become lower, from approximately 16 metric tons/day/meter to 14 metric tons/day/meter and the profiles become smooth. The channel bed slope at the beginning of the simulation in Reach 2 was 0.0004 m/m and at the end of the simulation the channel bed slope had flattened to 0.0007 m/m. The sediment transport rates in Reach 1 increase during the simulation, as does the channel slope from 0.0004 m/m to 0.0005 m/m. Reach 3 sediment transport rates increase during the simulation in the downstream end as lower end of the reach is eroded at the break in slope and the downstream end of Reach 3 becomes slightly steeper. The overall slope of Reach 3 remains constant at 0.0002 m/m. Erosion occurs at the convex portions of the channel profile (approximately 25,000 m) and deposits in the concave portion of the channel profile (approximately 15,000 m).

Susan Cundiff, P.E., CFM

Figure 11   Resulting bed and water-surface profiles for the mobile bed simulation in the conceptual model. This simulation had 1 cms/m, d_{50} of 0.5 mm, and used Engelund-Hansen sediment transport equation.

Figure 12   The resulting unit sediment transport rate for 1 cms/m, d_{50} fo 0.5 mm and Engelund-Hansen sediment transport equation.

Susan Cundiff, P.E., CFM

The results from the 5cms/m conceptual model execution again show that an increase in unit discharge shows a striking change in channel bed and water-surface elevations when comparing to the 1cms/m runs (**Figure 13**). **Figure 14** shows sediment transport rates are higher for the 5 cms/m simulation than the 1 cms/m by about 90 metric tons/day/meter in Reach 2. The channel bed and water-surface elevations show similar shapes as the previous runs as well as the sediment transport rate profiles have similar shapes. The channel bed slope increases to 0.0005 m/m in Reach 1 while the slope in Reach 2 decreases to 0.0005 m/m which is the same as Reach 1. The slope in Reach 3 increases from 0.0002 m/m to 0.0003 m/m. It is evident in this simulation that the bed slopes and water-surface profiles are reaching similar slopes throughout the entire study area as the model is approaching an equilibrium state (Schumm et al., 1984).
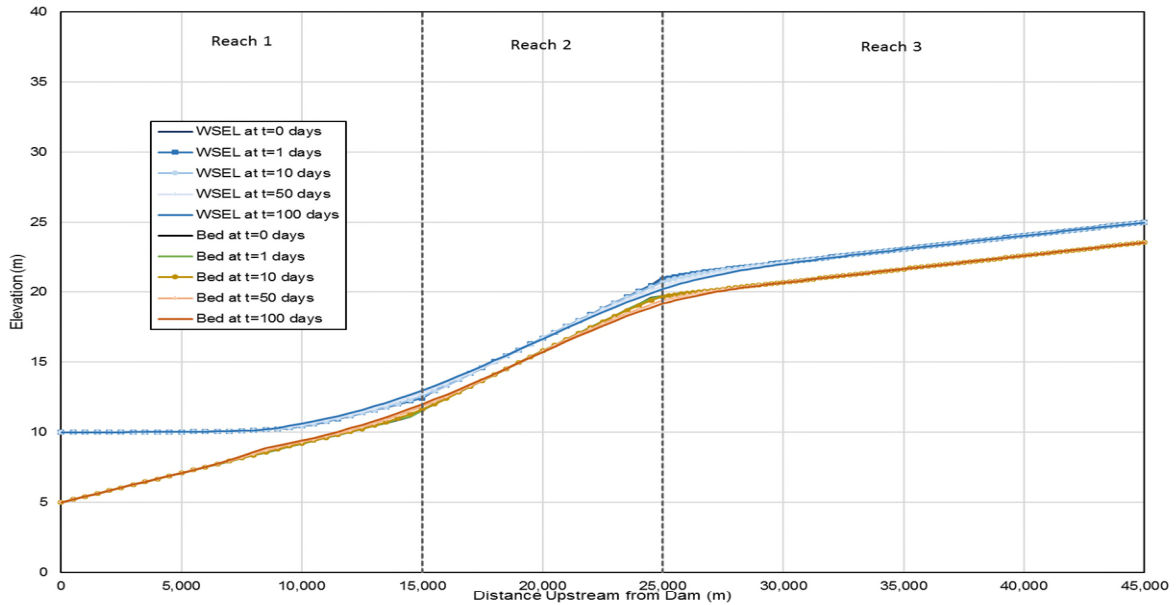

Figure 13   Resulting bed and water-surface profiles for the mobile bed simulation in the conceptual model. This simulation had 5 cms/m, d50 of 0.5 mm, and used Engelund-Hansen sediment transport equation.

Susan Cundiff, P.E., CFM

Figure 14   The resulting unit sediment transport rate for 5 cms/m, d_{50} fo 0.5 mm and Engelund-Hansen sediment transport equation.

The final conceptual model run at 10 cms/m shows the same trends as in the first 3 simulations but more pronounced. The channel bed at the Reach 2-Reach 3 transition lowers nearly 3 m (**Figure 15**) as the maximum sediment transport rate is approximately 100 m downstream of the Reach 2-Reach 3 break and is approximately 800 metric tons/day/meter at the start of the simulation (**Figure 16**). The sediment transport rates continue to be the highest in Reach 2 where the channel bed slope was the steepest at 0.0008 m/m. The resulting channel bed slope of Reach 2 is 0.0004 m/m. Interestingly, as the simulation progresses the sediment transport rates in Reach 2 drop while the sediment transport rates in Reaches 1 and 3 increase with time and in the downstream direction at the 100 day mark. The final channel bed slopes in these reaches are 0.0005 m/m and 0.0003, respectively.

         Susan Cundiff, P.E., CFM

Figure 15   Resulting bed and water-surface profiles for the mobile bed simulation in the conceptual model. This simulation had 10 cms/m, d_{50} of 0.5 mm, and used Engelund-Hansen sediment transport equation.
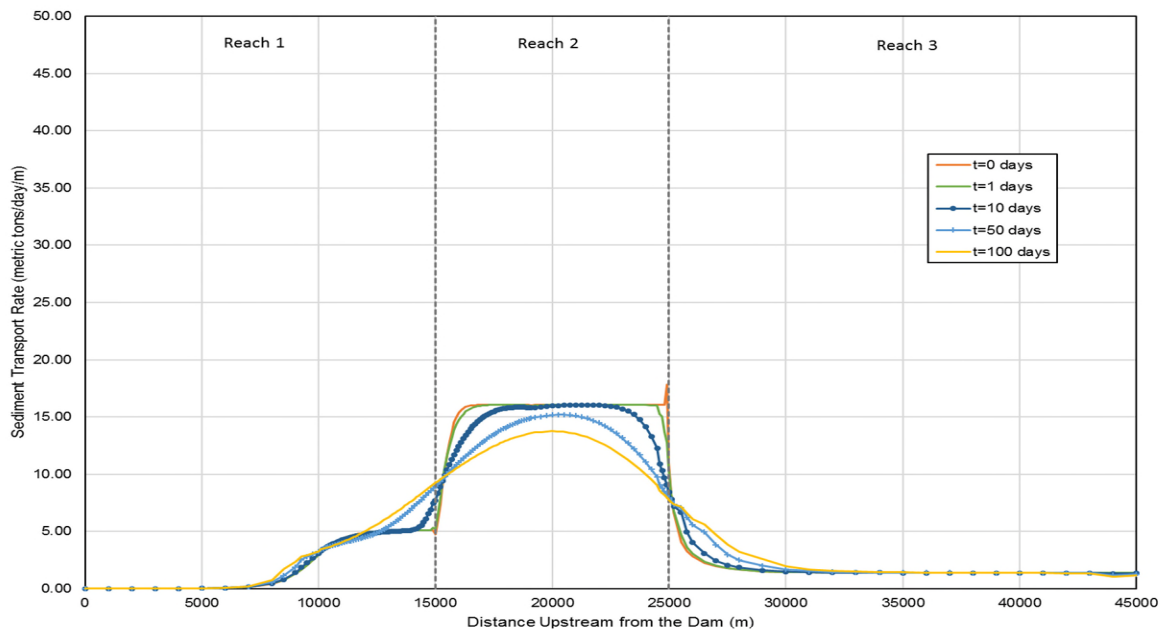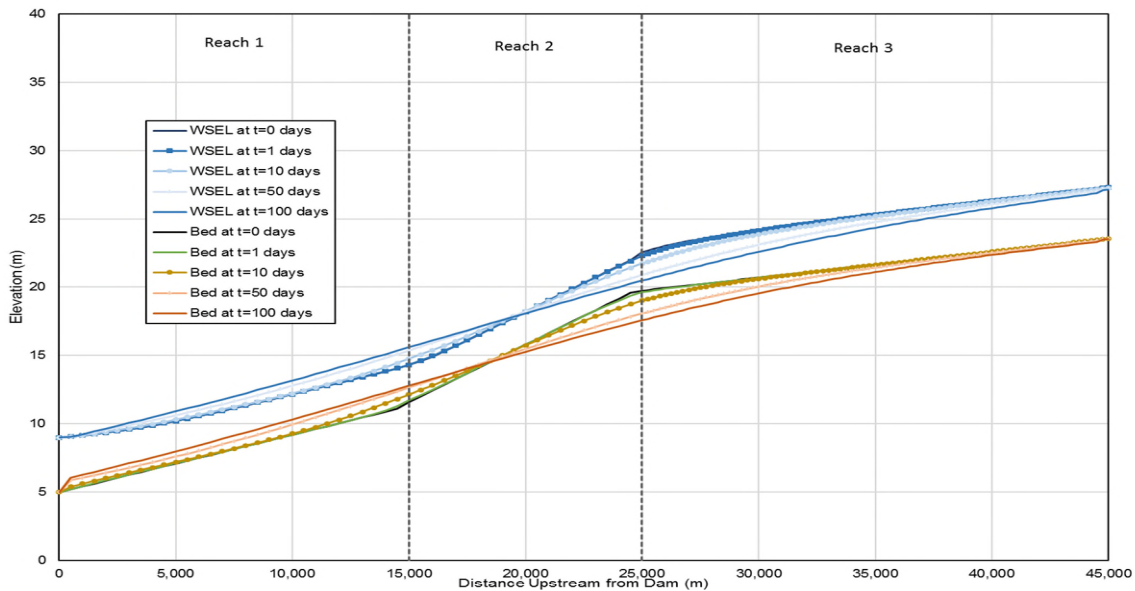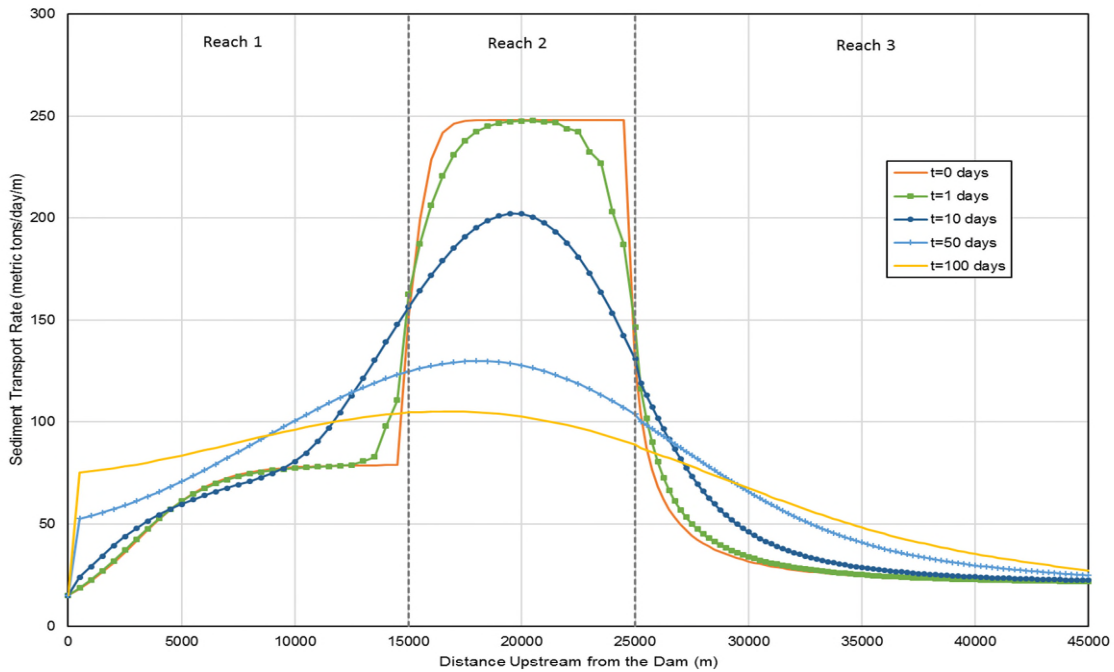

Figure 16   The resulting unit sediment transport rate for 10 cms/m, d_{50} fo 0.5 mm and Engelund-Hansen sediment transport equation.

Susan Cundiff, P.E., CFM

5.2   Results of Subsided Conceptual Model

To be consistent with the HEC-RAS models, the subsided conceptual model had the channel bed lowered in a similar magnitude and pattern as the Bypass System **(Figure 17)**. The downstream end maintained the same downstream channel bed elevation of 5 m and the middle of the channel profile, at 20,000 was lowered 3 m. As mentioned in Section 4.1, the starting slope at Reach 1 is 0.0003 m/m, at Reach 2 is 0.0008 m/m, and at Reach 3 is 0.0003 m/m. Reach 2 has a slight break in slope in the middle at station 20,000 m where the downstream portion is 0.0007 m/m and the upstream portion is 0.0009 m/m which is a result of the manner of the subsidence applied to this model where the most subsidence occurred at station 20,000 m.
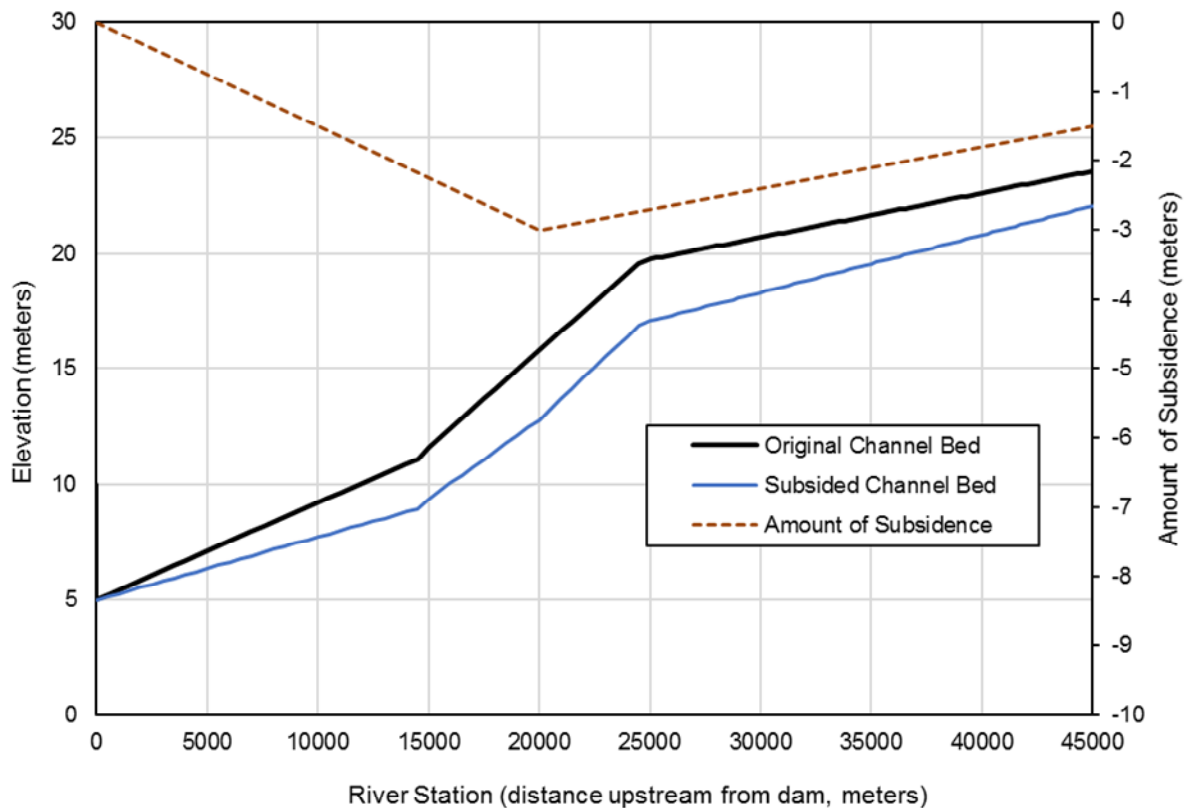
Figure 17   Initial channel bed and subsided channel bed for conceptual model. The brown dashed line demonstrates the amount of subsidence.

Susan Cundiff, P.E., CFM

The 1 cms/m simulation was executed for 100 days. The channel bed and water-surface elevation profiles show minimal erosion and sedimentation at the Reach breaks (**Figure 18**). The sediment transport rates are shown in **Figure 19**. The break in slope within Reach 2 is noticeable in the first 10 days of the simulation, and less so at the later reported timesteps. As time progresses, the starting sediment transport rates in Reach 2 decrease, from approximately 18 metric tons/day/meter to almost 13 metric tons/day/meter, as the channel slope decreases from 0.0008 m/m to 0.0007 m/m. The sediment transport rates increase with time at the Reach 1 to Reach 2 interface and at the Reach 2 to Reach 3 interface. The overall channel slopes of Reach 1 and Reach 3 remain constant, but some aggradation in the upstream end of Reach 1 is noticeable, about 0.5 m; and at the downstream end of Reach 3 about 0.5 m of degradation occurs.
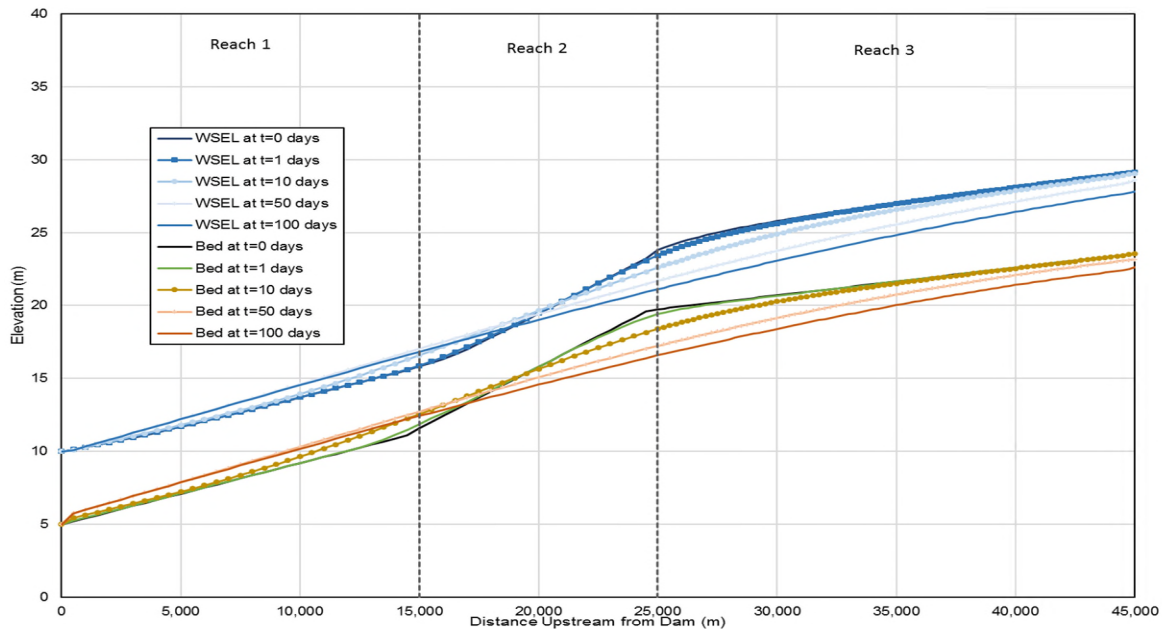

Figure 18   Resulting bed and water-surface profiles for the mobile bed simulation in the conceptual model with subsidence. This simulation had 1 cms/m, d_{50} of 0.5 mm, and used Engelund-Hansen sediment transport equation.

Susan Cundiff, P.E., CFM
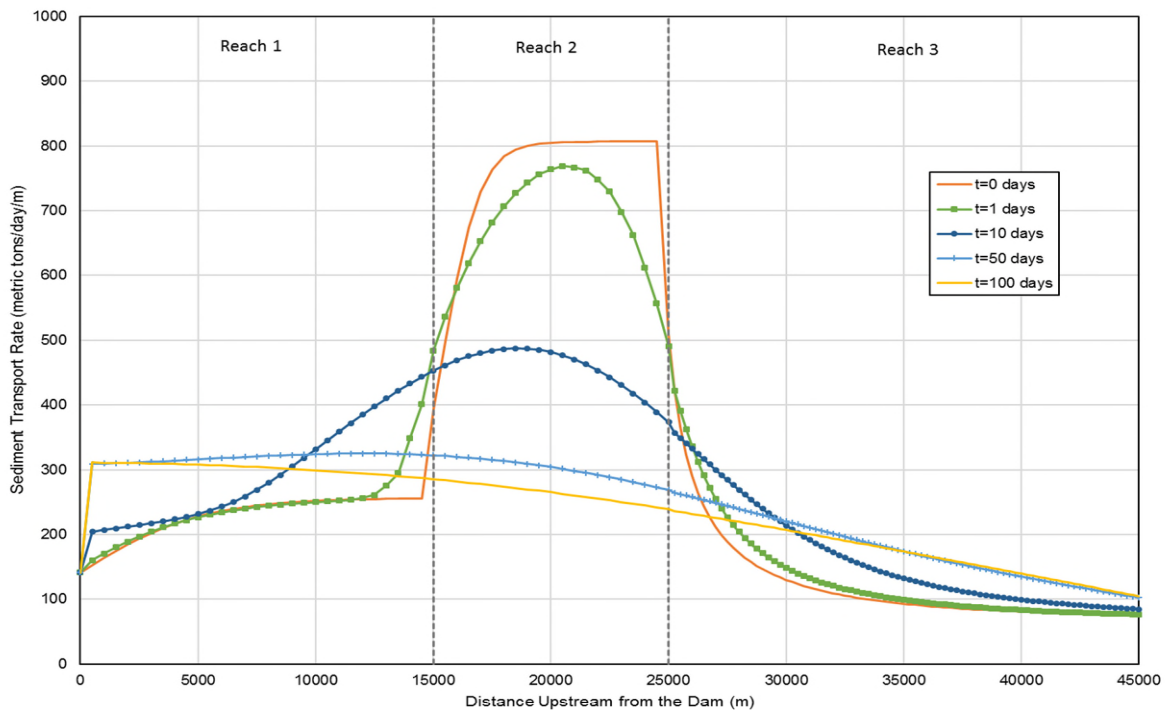
Figure 19   The resulting unit sediment transport rate for 1 cms/m, d_{50} fo 0.5 mm and
Engelund-Hansen sediment transport equation.

The subsided simple model was run with a unit discharge of 5 cms/m and the results show similar trends as the previous simulation at the lower unit discharges where channel bed and water-surface elevation profiles (**Figure 20**) continue to become more similar throughout the entire study area. **Figure 21** shows sediment transport rates are high in Reach 2, up to 278 metric tons/day/m at the beginning of the simulation. The sediment transport rates lower in Reach 2 as the simulation progresses and increase in Reaches 1 and 3 with a smoother, more symmetrical profile with the high point in Reach 2 at the end of the simulation. The end of simulation reach slopes are 0.0004 m/m, 0.0004 m/m, and 0.0003 m/m for Reach 1, Reach 2, and Reach 3, respectively.
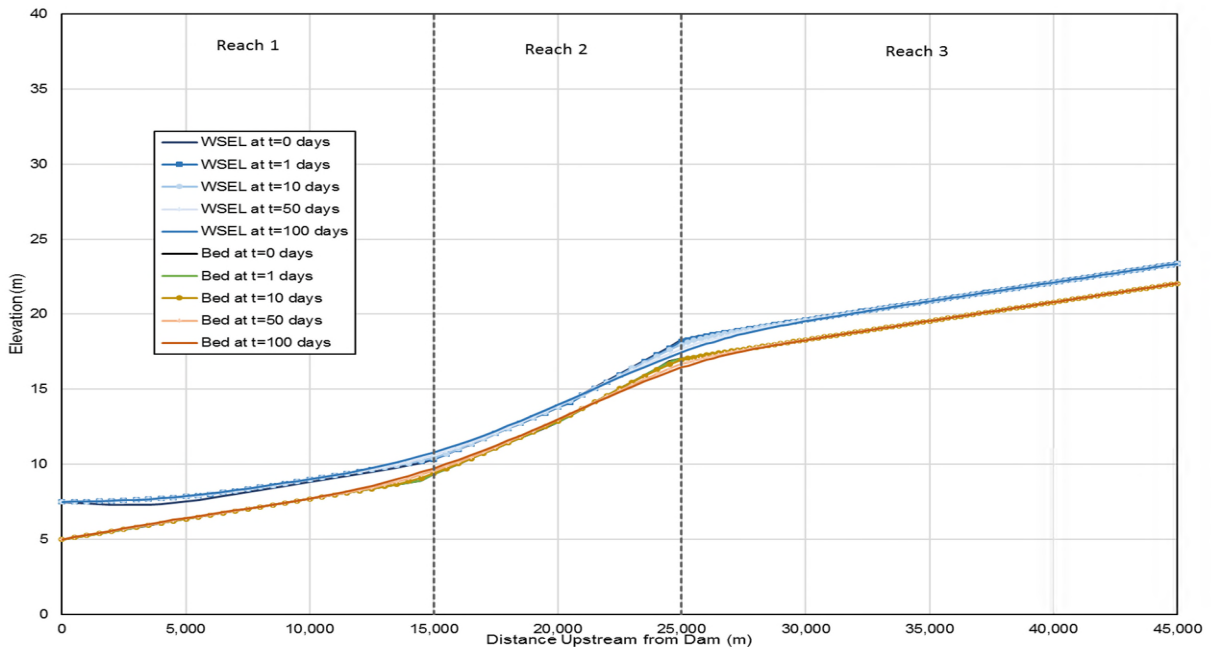
Figure 20   Resulting bed and water-surface profiles for the mobile bed simulation in the conceptual model with subsidence. This simulation had 5 cms/m, d_{50} of 0.5 mm, and used Engelund-Hansen sediment transport equation.

Figure 21   The resulting unit sediment transport rate for 5 cms/m, d_{50} for 0.5 mm and Engelund-Hansen sediment transport equation.

Susan Cundiff, P.E., CFM

The final subsided conceptual model simulation was executed for a unit discharge of 10 cms/m. The channel bed and water-surface elevations for this simulation show a nearly uniform slope for all the reaches (**Figure 22**). The final channel bed slopes are 0.0004 m/m, 0.0004 m/m, and 0.0003 m/m for Reach 1, Reach 2, and Reach 3, respectively. The area between Reach 1 and Reach 2 has almost 2 m of aggradation at the end of the simulation, while the area between Reach 2 and Reach 3 experienced just over 2 m of degradation. Reach 2 sediment transport rates (**Figure 23**) are as high as 900 metric tons/day/m and are reduced to about 400 metric tons/day/m after 10 days of simulation time. As time progresses, Reach 1 sediment transport rates increase by about 100 metric tons/day/m from the beginning of the simulation to the end. In Reach 3, the sediment transport rates at 100 days are slightly lower than at 50 days. This is because the channel bed slope was reduced enough that the transport capacity was reduced, thus creating a boundary condition establishing a lower sediment transport rate in Reach 3.
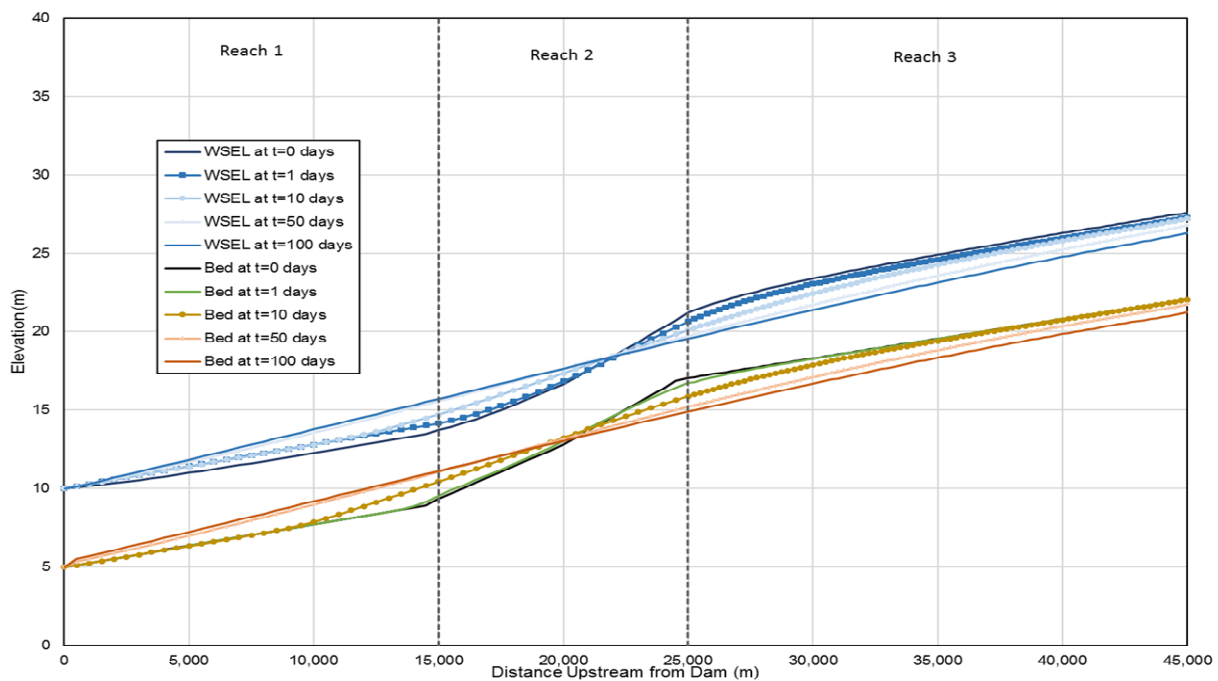
Figure 22   Resulting bed and water-surface profiles for the mobile bed simulation in the conceptual model with subsidence. This simulation had 10 cms/m, d_{50} of 0.5 mm, and used Engelund-Hansen sediment transport equation.
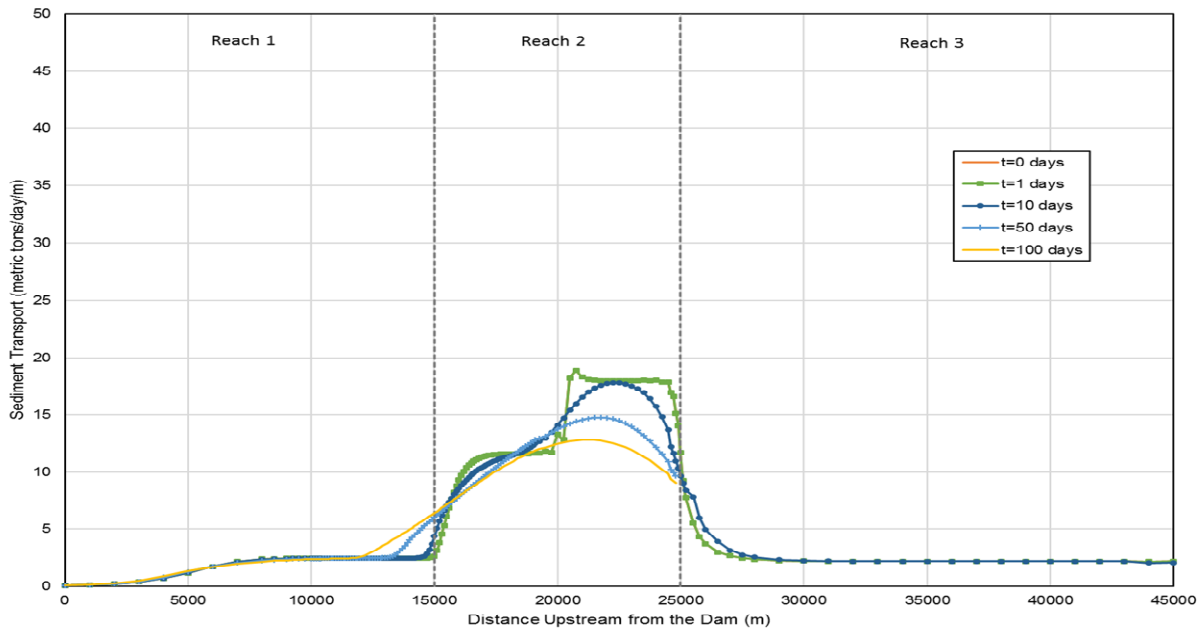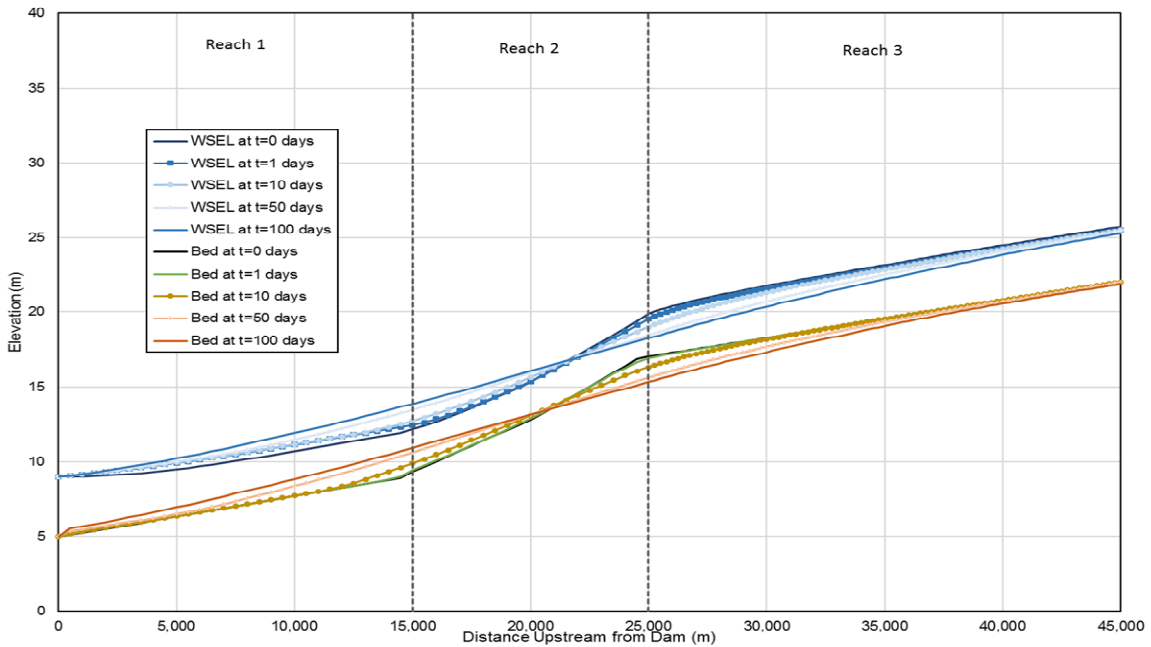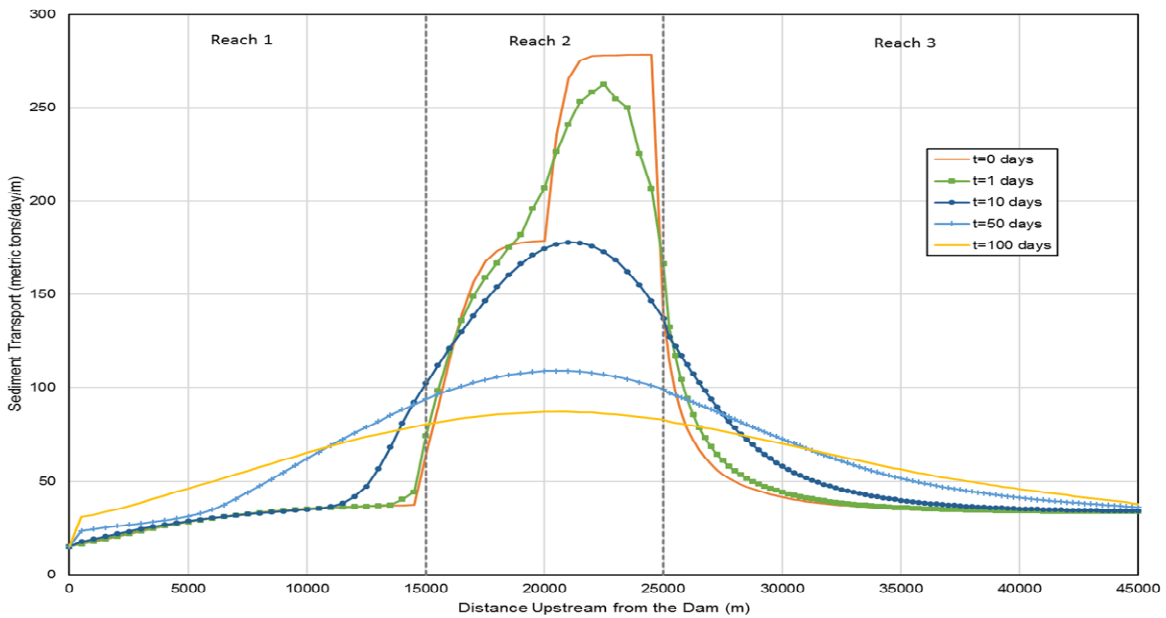
Susan Cundiff, P.E., CFM
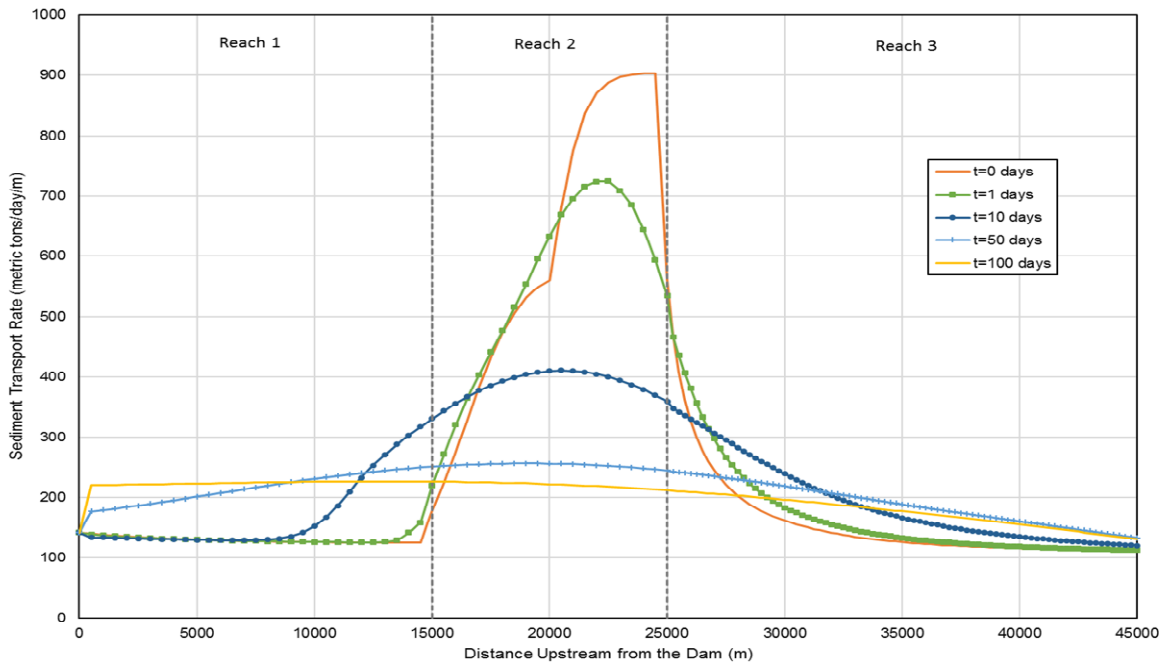
Figure 23   The resulting unit sediment transport rate for 10 cms/m, d_{50} for 0.5 mm and Engelund-Hansen sediment transport equation.

5.3   Comparison of Conceptual Model Results

Results from the No Subsidence and Subsidence conceptual models are compared to see the relative changes when subsidence is included. **Figure 24** shows sediment transport rates for both the Subsided and No Subsidence runs at five stations along the conceptual model for Day 0 of the simulation with the initial bed slopes. In Figure 24 the upstream end of the conceptual model reach, Sta 250+00 and Sta 300+00 the Subsidence runs had higher sediment transport rates than the No Subsidence runs because the bed slopes were steeper in that section. Alternatively, further downstream the No Subsidence run has higher sediment transport rates as the subsided bed slopes were reduced. **Figure 25**, **Figure 26** and **Figure 27** show results for Day 1, Day 10 and Day 50 results, respectively and show the same trends as in Figure 25 where the upstream two locations have sediment transport rates that are higher for Subsidence than No Subsidence runs. In **Figure 28**, Day 100, the bed profiles have changed enough that at all discharges and locations, except Sta 300+00, the No Subsidence runs have the higher sediment transport rates.

Susan Cundiff, P.E., CFM

Figure 24   Comparison of sediment transport rates from the Simple Model (No Subsidence) and the Subsidence Simple Model (Subsidence) on Day 0 on the simulation at various stations.
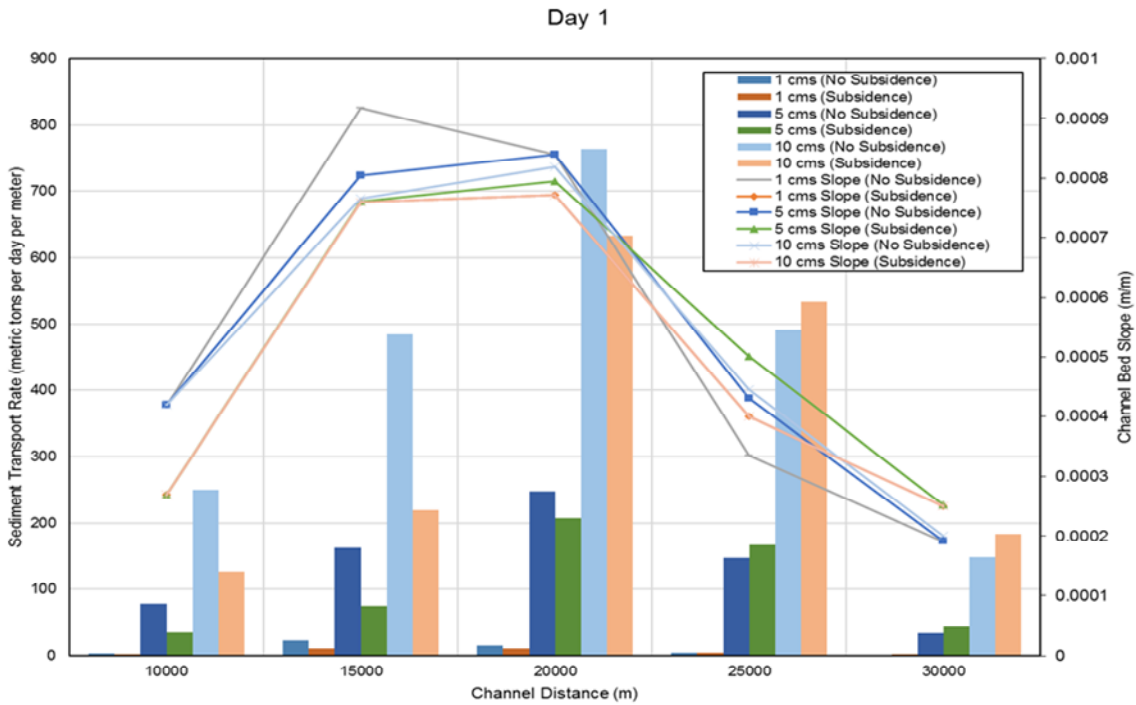
Figure 25   Comparison of sediment transport rates from the Simple Model (No Subsidence) and the Subsidence Simple Model (Subsidence) on Day 1 on the simulation at various stations.

Susan Cundiff, P.E., CFM
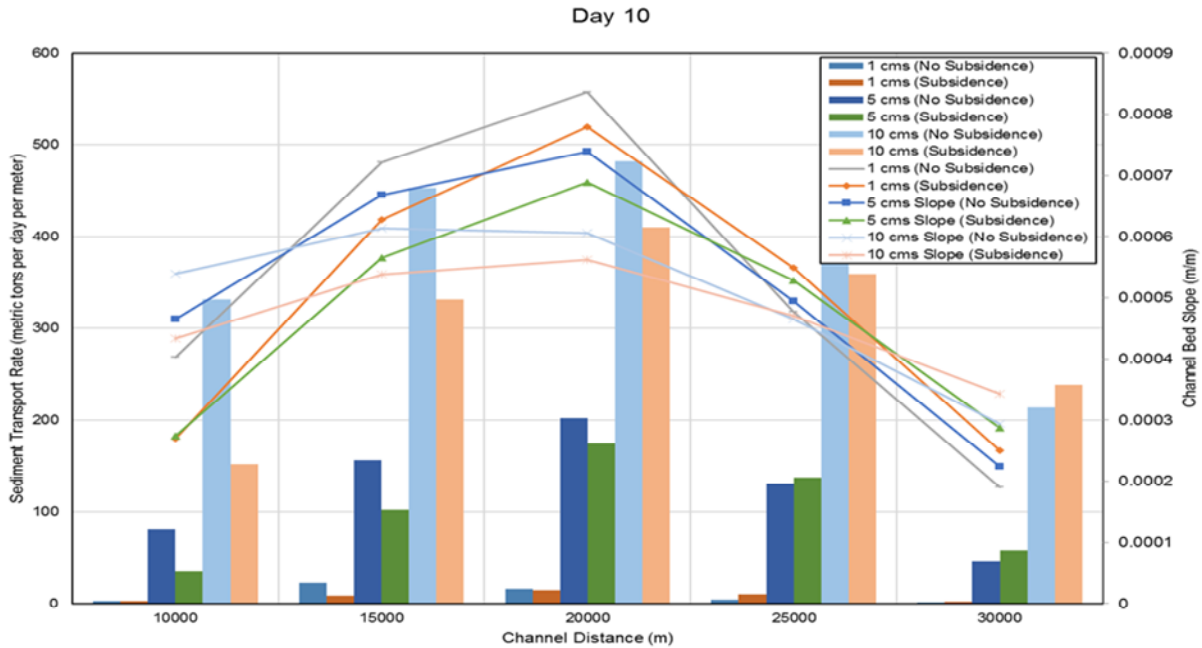
Figure 26   Comparison of sediment transport rates from the Simple Model (No Subsidence) and the Subsidence Simple Model (Subsidence) on Day 10 on the simulation at various stations.
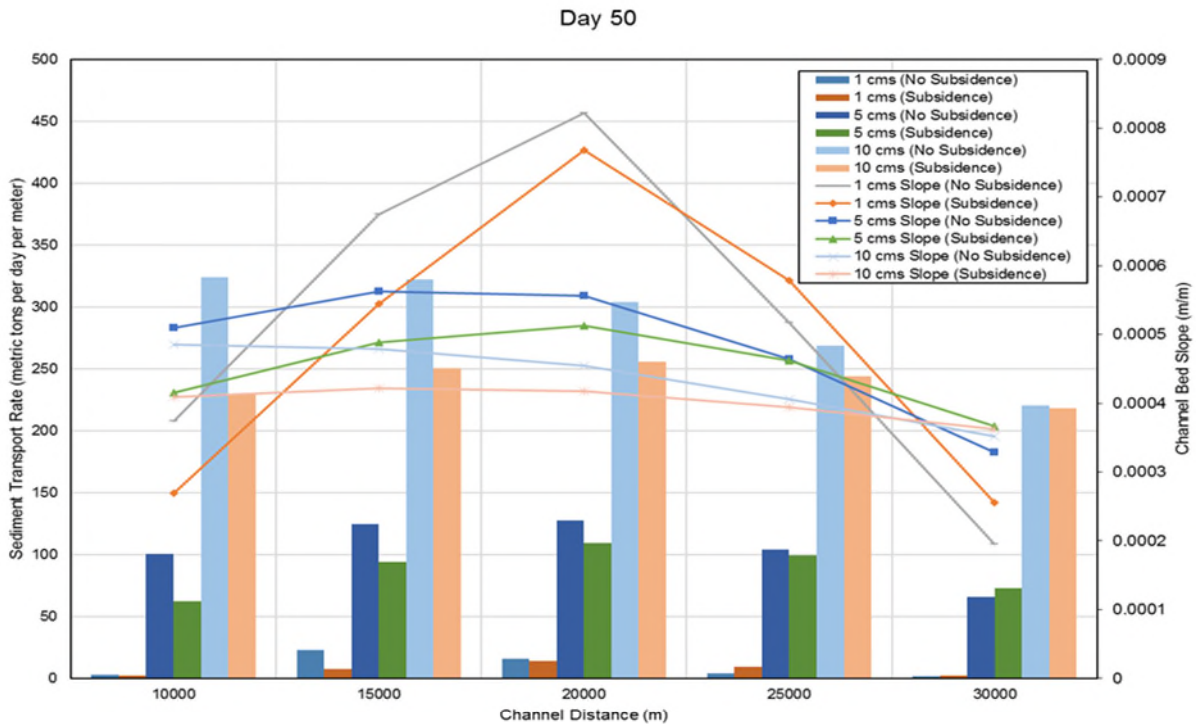
Figure 27   Comparison of sediment transport rates from the Simple Model (No Subsidence) and the Subsidence Simple Model (Subsidence) on Day 50 on the simulation at various stations.
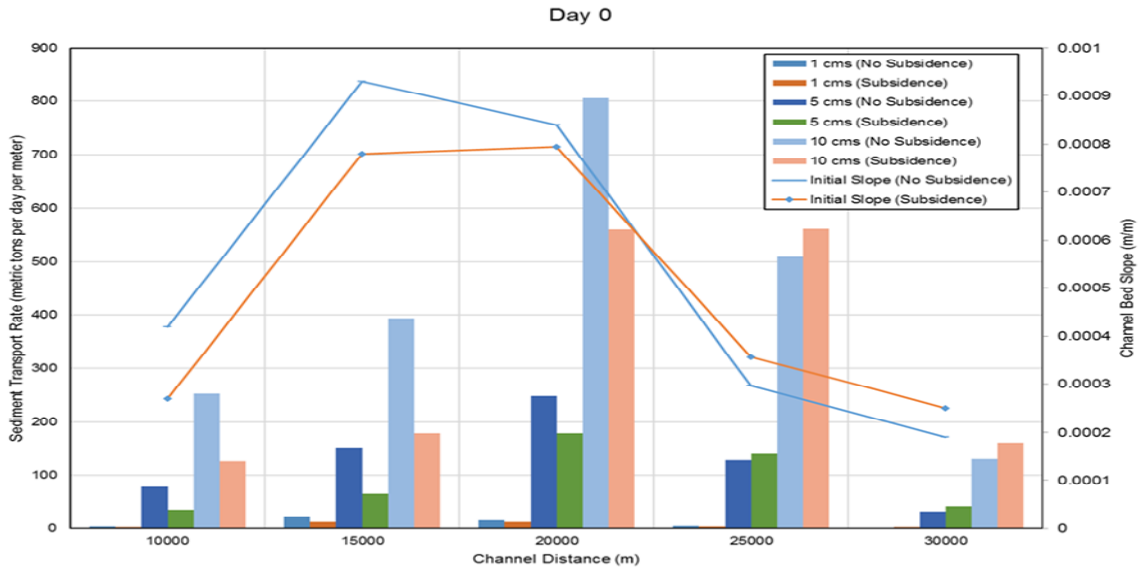
Susan Cundiff, P.E., CFM
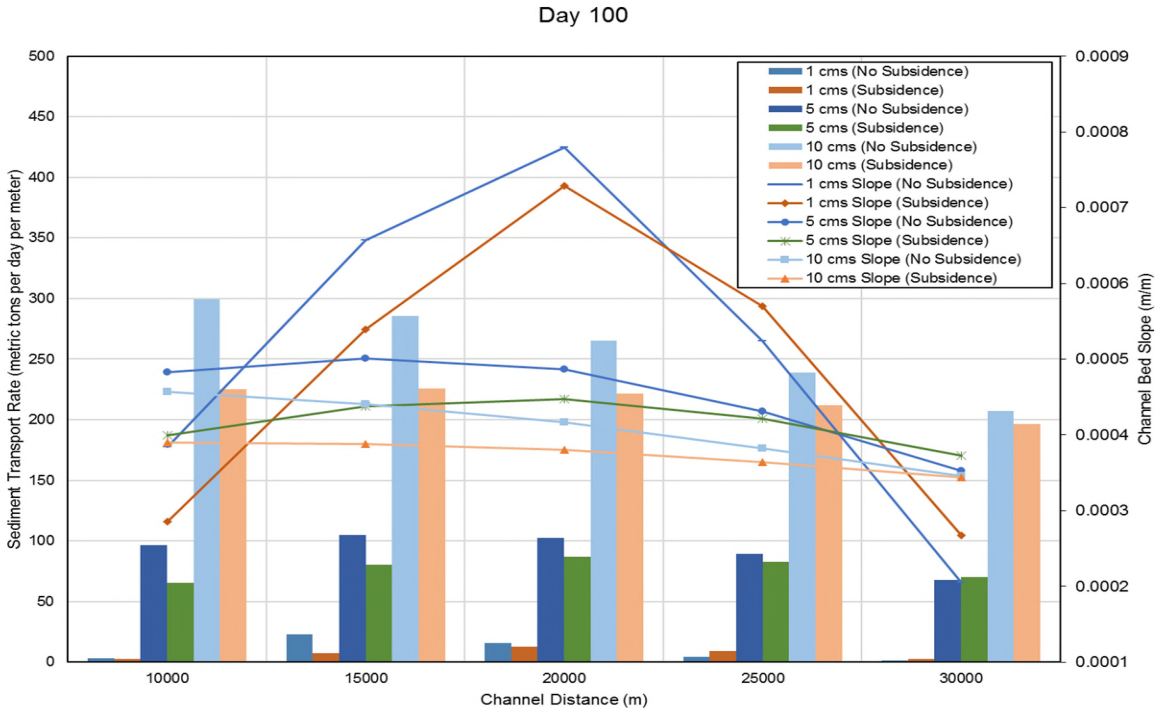
Figure 28   Comparison of sediment transport rates from the Simple Model (No Subsidence) and the Subsidence Simple Model (Subsidence) on Day 100 on the simulation at various stations.

5.4   Results of the HEC-RAS Mobile Boundary Model (No Subsidence)

The first model developed for the San Joaquin Bypass system was executed for the 13-year simulation period without applying the annual subsidence rate is referred to as No Subsidence. The No Subsidence model will act as the control when comparing to the results from the subsidence simulations. Five locations were selected along the profile to study the sediment transport loads in more detail in the Bypass system. The cross sections were selected at interesting points along the subsidence profile, and outside of the direct influence of tributaries, control structures and bridges (**Figure 29)**. Figure 29 shows the beginning of simulation and end of simulation mean bed elevations along the Bypass with water-surface profiles of 4,500 cfs, which are a target discharge for the Program. In the upstream section from about station 2,400+00 feet to the upstream end the channel beds are very similar with minor areas of erosion and deposition. Moving downstream from station 2,400+00 to 1,900+00 the model predicts erosion. This is consistent with real life as current conditions show much incision in this reach (Tetra Tech Inc. , 2015a). The Fresno River contributes occasional flows and sediment to the Bypass at approximately 1,900+00. The reach from the Fresno Slough to Ash Slough (1,622+00) show slight

but consistent degradation. From about 1,310+00 to 910+00 this reach shows aggradation. The reach just downstream of the Merced National Wildlife Refuge (MNWR) Weir, station 740+00 to station 650+00 experiences minimal degradation and the rest of the downstream portion of the channel has essentially the same channel bed indicating equilibrium.
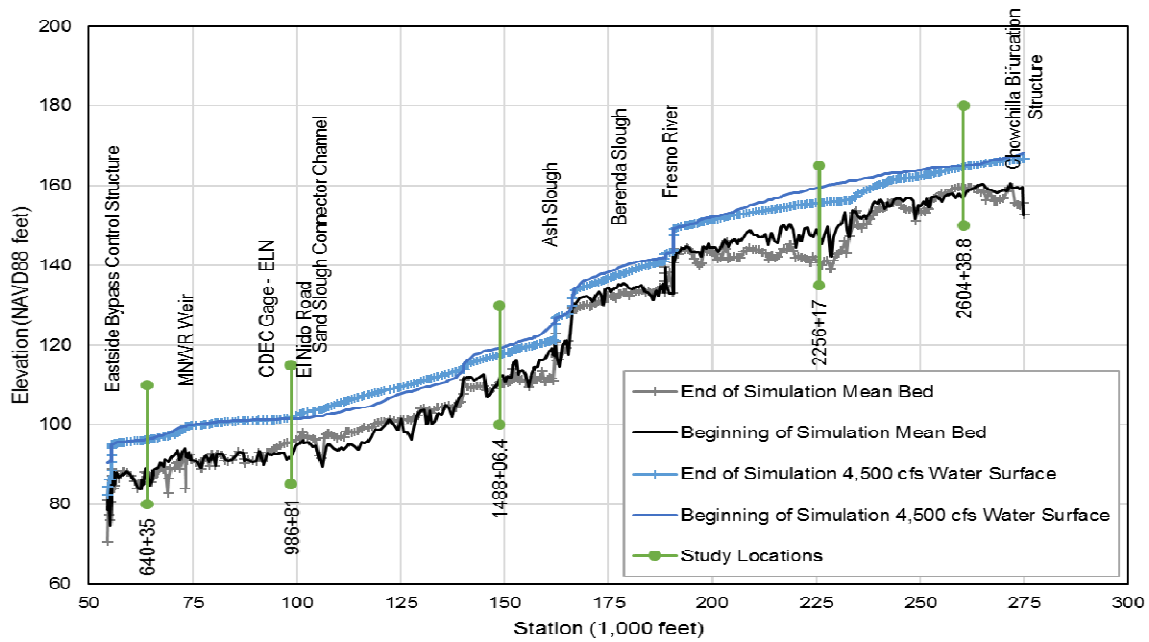
Figure 29   Mean Bed Elevations and 4,500 cfs Water-surface elevations for the
beginning and end of the No Subsidence simulation.

Figure 30 shows the cumulative channel mass change of sediment, in tons, for the duration of the simulation. The cumulative mass bed change is cumulative in time, but not in space. The cumulative mass bed change profile shows more negative net changes in the upper half of the Bypass System. A negative net change in sediment indicates erosion. Cross Section 2604+38.8 does show a positive value of 20,500 tons and this correlates to a small area of deposition in the channel bed profile in Figure 29. Cross Section 2256+17 is in the reach of the Bypass where significant amounts of erosion occurred during the simulation (Figure 29). The cumulative mass change at XS 2256+17 is about -36,700 tons of sediment. The next downstream studied cross section is XS 1488+06.4 which is downstream of the Fresno River and Ash Slough tributaries. The cumulative mass change of sediment at XS 1488+06.4 is about -7,800 tons. This cross section is in the steepest part of the bypass channel and downstream of the tributaries where it shows net degradation. The next downstream detailed study location is XS 986+81 and is just

downstream of El Nido Road and the confluence of Reach 4A. This location is in the backwater effects of the MNWR weirs and cause much deposition. A positive net difference at XS 986+81 of 195,100 tons is consistent with the deposition that occurs in this location during the No Subsidence simulation (Figure 29). The downstream most cross section that was selected for detailed analysis is XS 640+35. This cross section has a cumulative mass bed change of -4,700 tons and is consistent with the minimal channel bed elevation changes as shown in Figure 29.
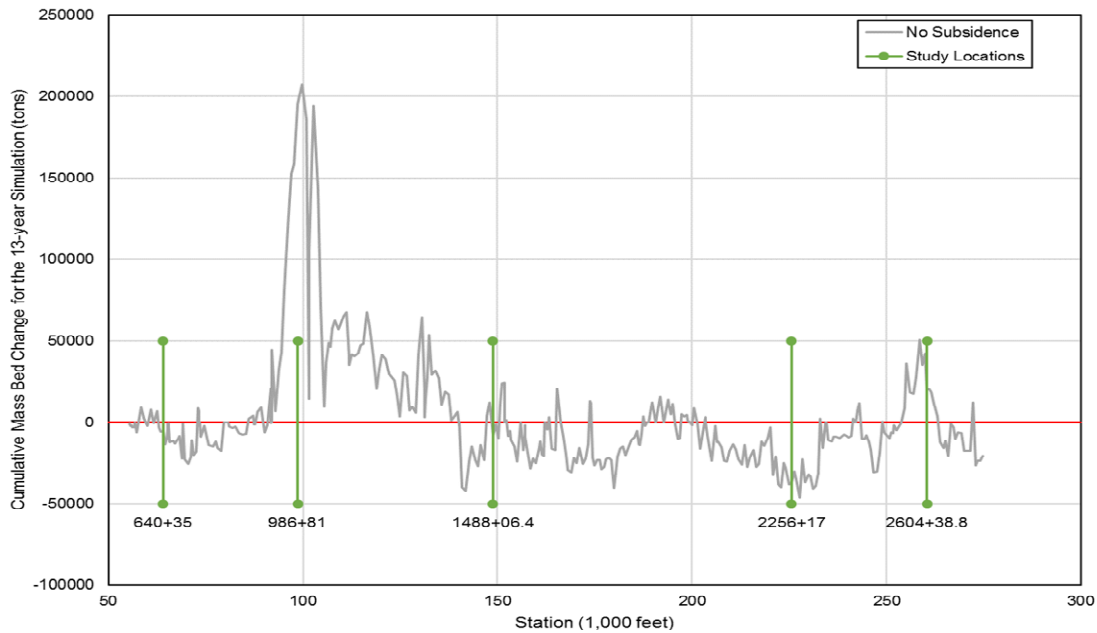
Figure 30   Cumulative mass bed change of sediment in tons for the 13-year No Subsidence simulation.

5.5   Results of the HEC-RAS Mobile Boundary Model (Subsidence)

The second model executed was the version with the annual subsidence rate applied incrementally (Subsidence). This version of the model was incrementally subsided at each cross section for each time step of the simulation with its unique rate as described in Section 4.2.2. The final mean bed elevations for the beginning and end of simulation are shown in **Figure 31**. While the end of simulation profile is lower in all locations and the amount of subsidence that has occurred is evident, the greatest difference between the two profiles is the center of the profile

between Fresno River (1900+00) and Ash Slough (1622+00). The least amount of difference is on the ends, consistent with Figure 6. It is difficult to determine exactly how much of the channel is experiencing deposition based on the beginning and final profiles because of the overall channel lowering. Consistent with the end of simulation profile in Figure 29, the end of simulation profile shows less vertical variability (i.e. pools and riffles) of local hydraulic controls than the
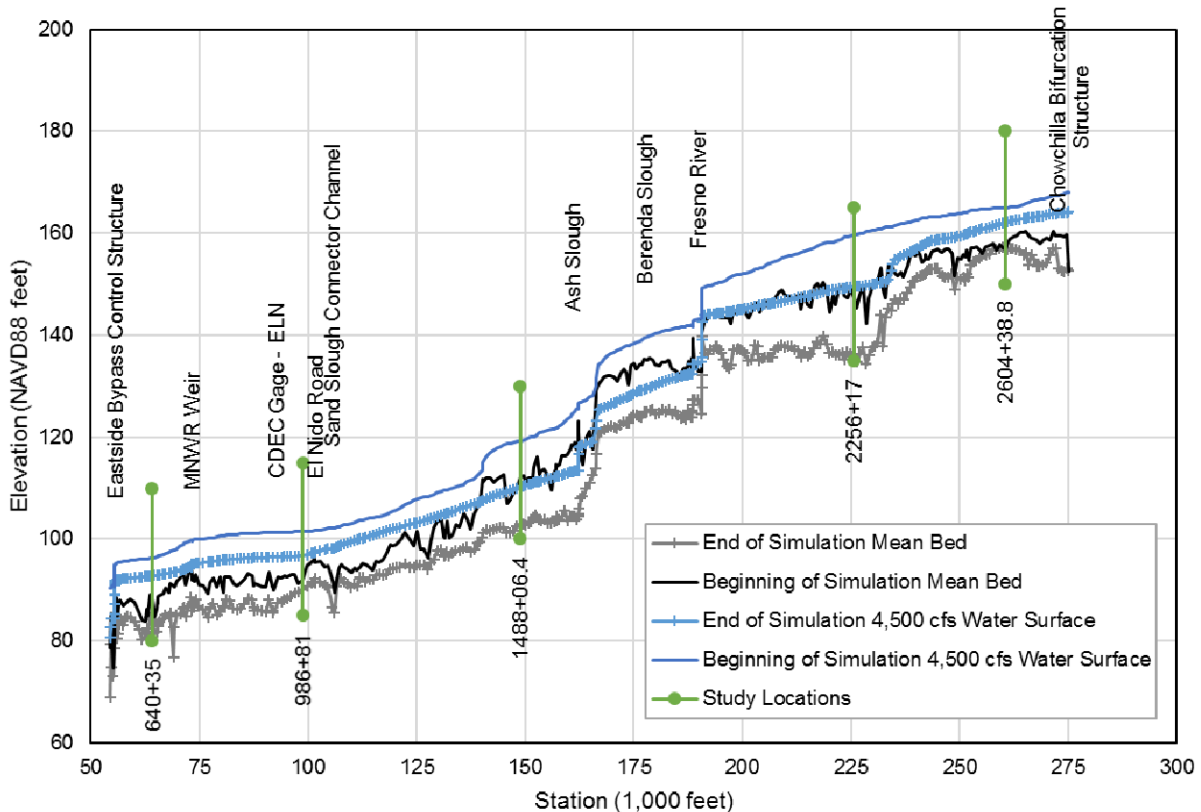
Figure 31   Mean Bed Elevations and 4,500 cfs Water-surface elevations for the beginning and end of the Subsidence simulation.

starting mean bed elevation profiles.

Figure 32 shows the cumulative channel mass change of sediment in tons for the 13-year simulation. Like the No Subsidence run, the upper half of the Bypass System shows a net negative mass bed change. While much of the upper half has net negative bed mass changes, the section at XS 2604+38.8 has positive 18,600 tons mass bed change, and is consistent with the aggradation that appears to have occurred in that section of the reach. Because the subsidence has increased the slope, the amount of mass bed change at XS 2256+17 is -42,800 tons and is in the reach with the most erosion. Cross section 1488+06.4 is located in the center of the reach from about 1800+00 to 980+00 where the cumulative mass bed change transitions from negative

to positive and has a value of 23,900 tons, which is a bit higher than the expected average amount. Cross section 986+81 is in the area downstream of El Nido Road and the confluence with Reach 4A and is in the backwater zone from the MNWR weirs. It has an extremely high cumulative mass bed change of 160,400 tons. Again, XS 640+35 has approximately a zero net cumulative mass bed change with a value of -800 tons of sediment for the entire 13-year simulation.
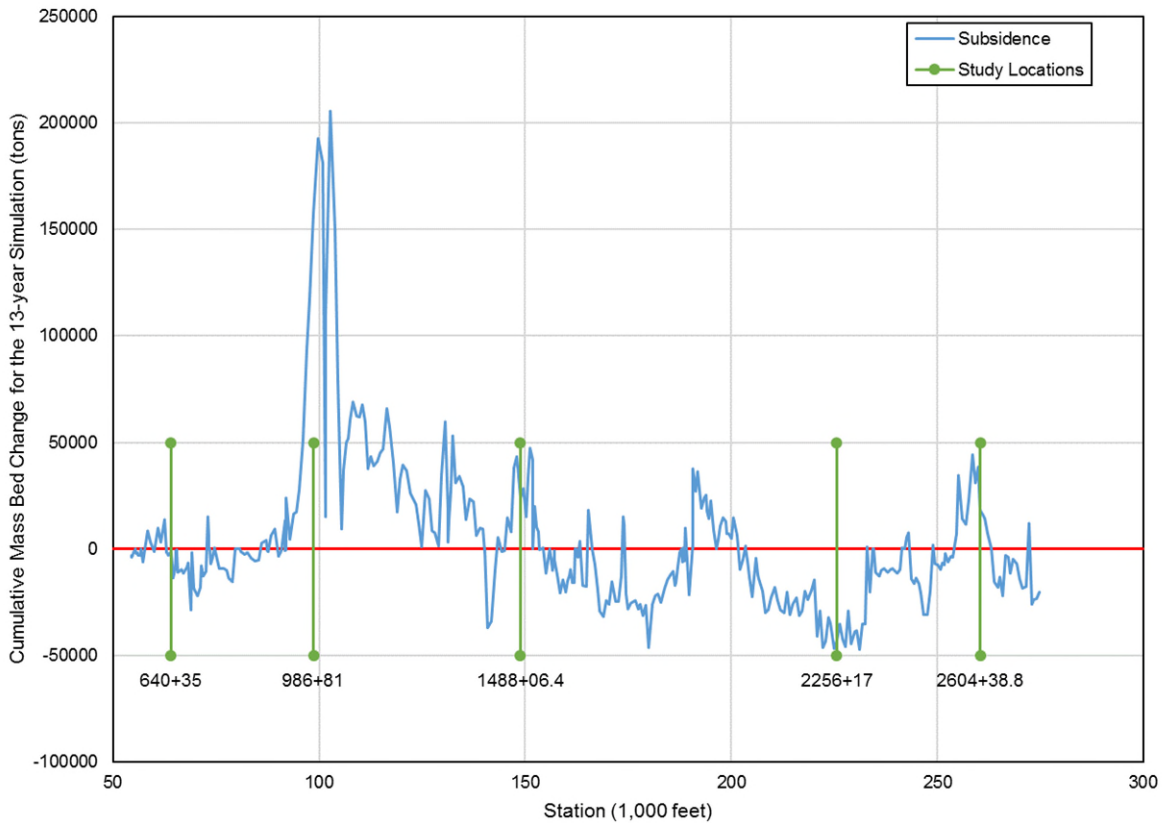
Figure 32   Cumulative mass bed change of sediment in tons for the 13-year Subsidence simulation.

5.6   Comparison of Mobile Boundary Model Results

The results from the two model runs are compared to understand the relative changes caused by subsidence. **Figure 33** compares the cumulative mass bed change for the No Subsidence and Subsidence runs for the entire Bypass System with the subsidence profile for comparison. Results show that the cumulative mass bed change is typically less than zero when the amount of subsidence increases in the downstream direction. The reach surrounding XS 2604+38.8 shows

Susan Cundiff, P.E., CFM

Figure 33   Comparison of the Cumulative Mass Bed Change in tons for the duration of the 13-year simulation for the No Subsidence and Subsidence.

a positive mass bed change which is also located at a location along the subsidence profile where the amount of subsidence decreases in the downstream direction, from -2.8 ft to -2 ft. As the amount of subsidence decreases in the downstream direction, from about 1500+00 to 820+00 the cumulative mass bed change becomes positive. As the subsidence profile flattens out the cumulative mass bed change values approach zero tons. On the upstream side of the Bypass System, or the falling limb of the subsidence profile, the Subsidence runs have more negative cumulative mass changes. Values for the Subsidence run for the reach from the upstream end to about 200+00 show up to 11,500 tons (**Figure 34**) more of a negative cumulative mass bed change than the No Subsidence run demonstrating that when accounting for the subsidence erosion is more likely. From about 200+00 to 128+00, the reach that travels through the epicenter of the subsidence will have up to 31,700 tons (Figure 34) more cumulative mass bed change in the Subsidence run than the No Subsidence run agreeing with the work from (Swanson, 1998) that sags in channel profile slopes will reduce capacity and increase sedimentation. The reach from about 128+00 and downstream shows that while the amount of subsidence is not

insignificant, approximately 6 feet, it is fairly uniform and thus the difference of cumulative mass bed changes between Subsidence and No Subsidence runs is fairly close with the exception of cross section just downstream of XS 986+81 (nearly 70,000 tons less). A notable thing is that anytime the total amount of subsidence sharply decreases the amount of cumulative mass bed change becomes positive, indicating deposition. Although XS 986+81 does not have a drastic decrease in the total amount of subsidence as the other locations mentioned, this cross section and the next one directly downstream are more effected by the backwater that is becoming more severe from the subsidence.

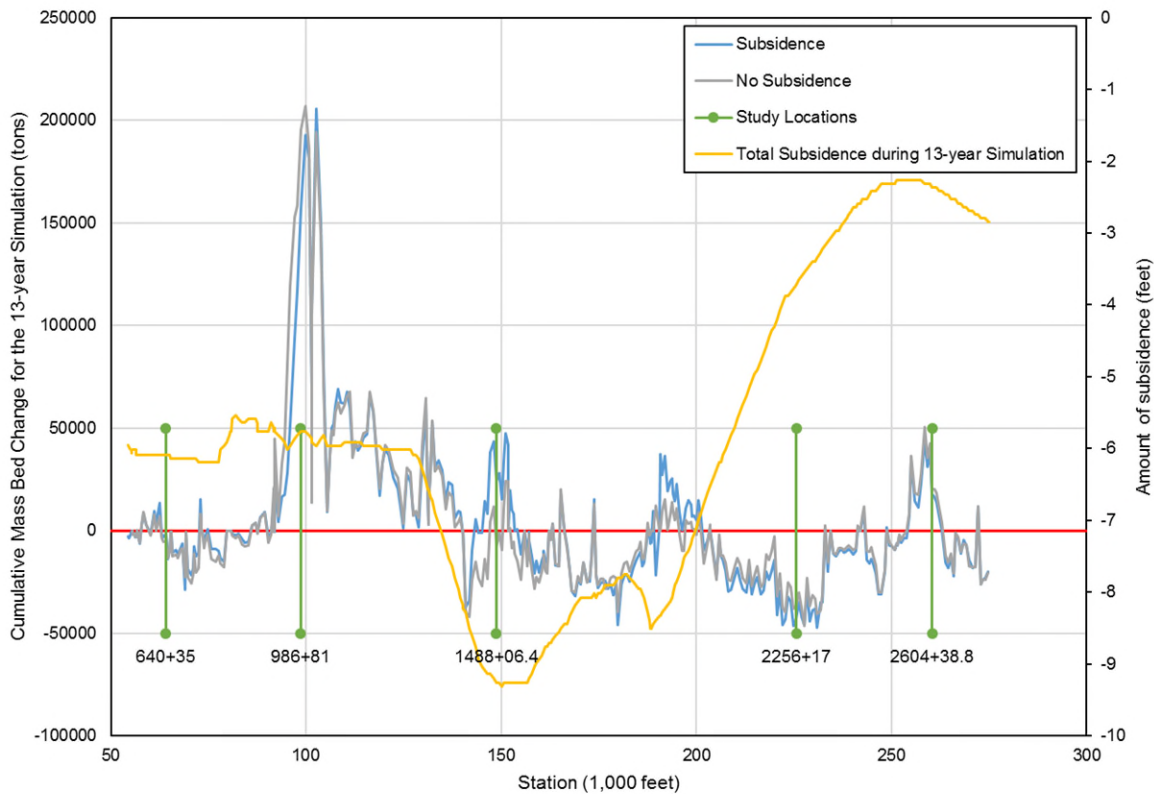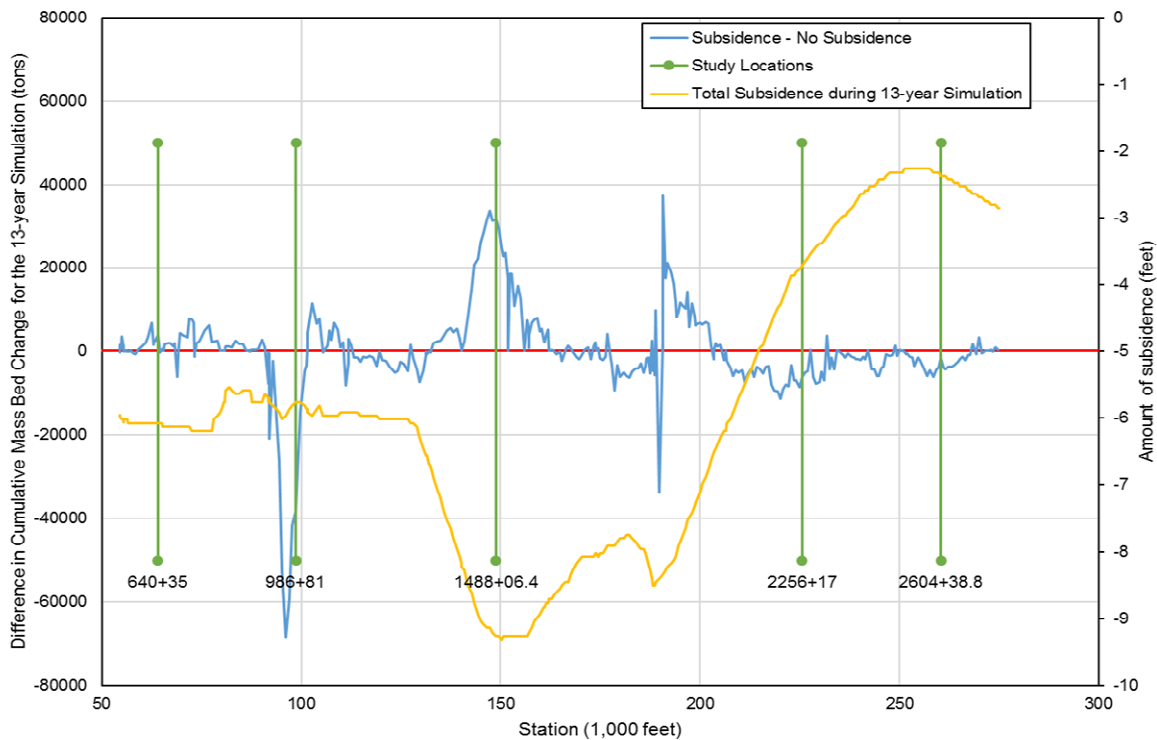Figure 34   Difference in the Cumulative Mass Bed Change in tons for the duration of the 13-year simulation for the No Subsidence and Subsidence.

Figure 35 shows the absolute mean effective invert change in feet for the Bypass System and the five study locations for the No Subsidence and Subsidence runs. Cross Section 2604+38 has a mean effective invert change of 2.13 feet, and -0.48 feet for No Subsidence, and Subsidence,

Susan Cundiff, P.E., CFM

respectively. As with the cumulative mass bed change comparison (Figure 33), the reach from the upstream end to about 200+00 shows negative changes except for the are in the immediate area of the XS 2604+38 where the total amount of subsidence shows a small reduction. Cross section 2256+17 has a net lowering of the mean effective invert of 6.58 feet, and 11.69 feet for the No Subsidence and No Subsidence runs, respectively. Sta 1488+06 has a mean effective invert change of -1.71 feet and -9.29 feet, for the No Subsidence and Subsidence runs, respectively. Sta 986+81 has a mean effective invert change of 3.65 feet and -1.98 feet for the No Subsidence and Subsidence runs. Cross section 640+35 shows a mean effective invert lowering of 0.25 ft for the No Subsidence run and the Subsidence run shows lowering of 3.98 feet.

Figure 35   Absolute Mean Effective Invert Change in feet for the duration of the 13-year simulation for the No Subsidence, and Subsidence models.

Because the mean effective invert change includes the amount of subsidence, an adjustment was made to the Subsidence runs to remove the amount of subsidence that occurred during the 13-year simulation. **Figure 36** shows the subsidence adjusted, or relative mean effective invert change in feet for the Bypass System and at the five study locations. When adjusting for

subsidence (Figure 36) the mean effective invert change shows aggradation of nearly 2 feet, 1.89 feet at Sta 2604+38 compared to 0.48 feet of degradation with no adjustment for subsidence. The subsidence adjusted mean effective invert change at Sta 2256+17 is -7.98 feet instead of -11.69 feet. In the center of the reach at Sta 1488+06 the relative mean effective invert change is -0.04 feet compared to the unadjusted amount of -9.29 feet. Sta 986+81 has value of 3.78 feet of aggradation compared to the unadjusted mean effective invert change of -1.98 feet. The downstream end, Sta 640+35 shows 2.1 feet of aggradation while the unadjusted mean effective invert change shows -3.98 feet.

Figure 36   Subsidence Adjusted Mean Effective Invert Change in feet for the duration of the 13-year simulation for the No Subsidence, and Subsidence models.

Bed response as demonstrated by relative mean effective invert changes in Figure 36 shows that aggradation and degradation trends are similar for the entire Bypass System. In locations on the steep side of the subsidence profile, from the upstream end to 200+00, the Subsidence run predicts more bed erosion, by up to 2 feet more than the No Subsidence run (**Figure 37**). From

about 200+00 to 128+00, in the sag of the subsidence profile, the Subsidence model run generally shows more aggradation, with values of up to 2.1 feet more. From 128+00 to the downstream end, shows significant deposition based on the relative mean effective invert change under the Subsidence run, up to 2.9 feet of deposition.
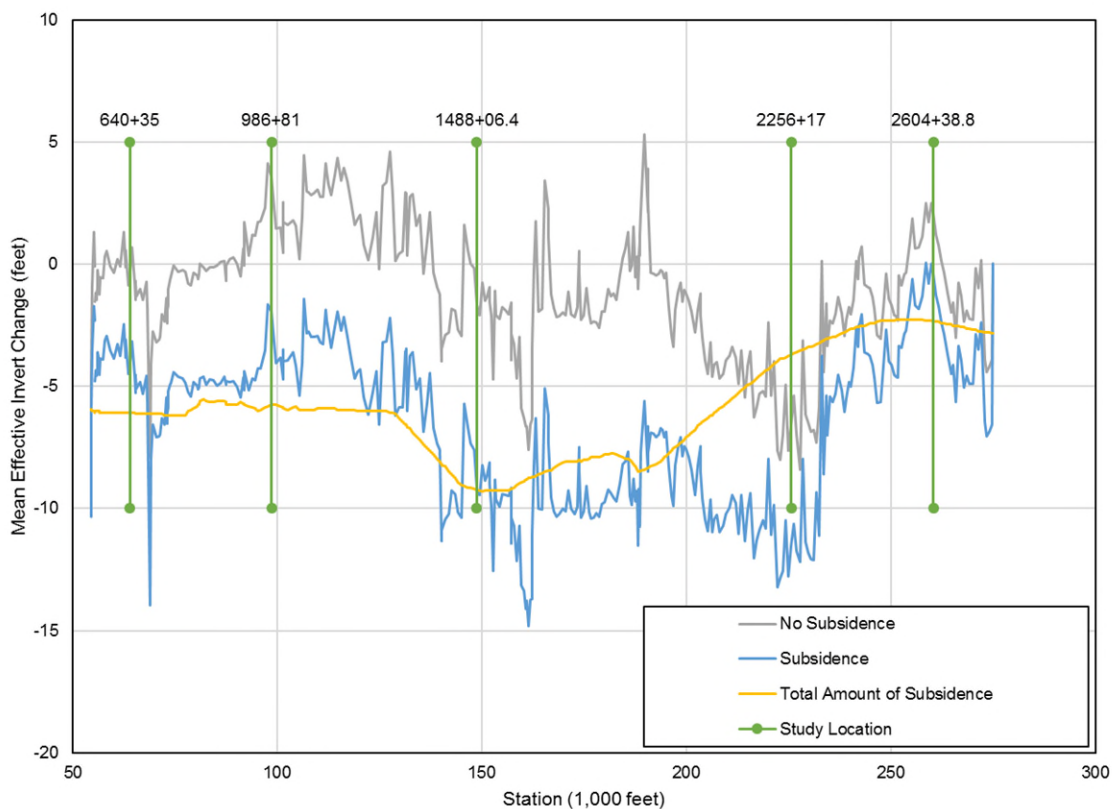

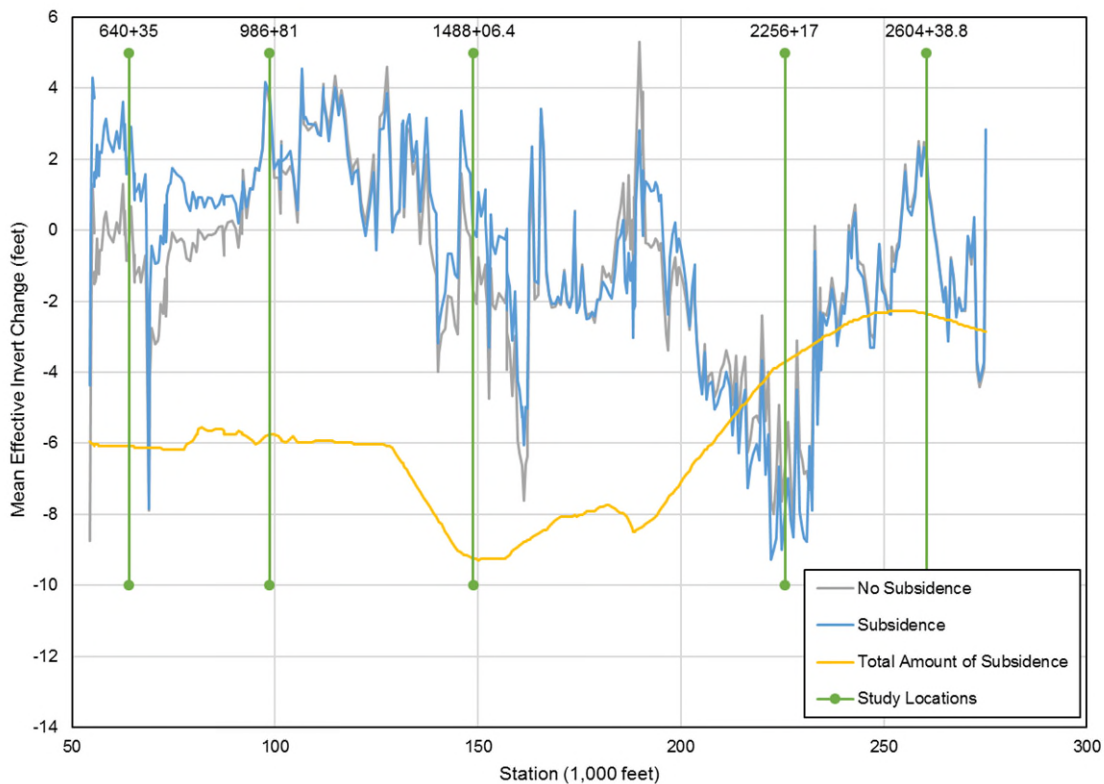Figure 37   Difference in the Relative Mean Effective Invert Change in feet for the duration of the 13-year simulation for the No Subsidence, and Subsidence models.

This study shows that the bed response to land subsidence can be significant and that this makes it appropriate to account for subsidence when modeling mobile boundary models in areas that experience subsidence. The length of the simulation, rate of subsidence and end goal of the mobile boundary model must be considered when determining whether subsidence should be modeled. The steps to set up a mobile boundary model are plentiful. The additional steps to prepare a mobile boundary model for subsidence are not trivial. HEC-RAS 5.0.5 currently does not apply subsidence to certain features of the cross sections, for example, ineffective flows, levees, internal bridge cross sections. If these features are key to accurate hydraulics in the cross sections of a model, adjustments to these must be made or the subsidence will render the

Susan Cundiff, P.E., CFM

hydraulics from subsided cross sections useless and yield meaningless results. Results on the upstream side of the subsidence induced sag may be dampened as this section of the river has already experience tremendous amounts of subsidence since the beginning of the Bypass System construction. That section of channel is most likely responding to this perturbation and both the No Subsidence and Subsidence runs are predicting erosion.

Things to consider before embarking on mobile boundary modeling with subsidence are:

- Length of simulation.
- Rate of subsidence.
- Shape of subsidence occurring on the river system.
- The point at which a system has already subsided.

The answer to each of those considerations will guide the modeler to which technique will be more appropriate for modeling subsidence. Long term simulations, perhaps longer than 13-years, would possibly benefit from the incremental subsidence. The locations that had lower rates differential rates of subsidence had fewer differences between the Subsidence and No Subsidence runs, meaning, if an area does not have areas of rapid subsidence, there is less benefit to the extra effort of developing the subsiding model.

7. Conclusions

By using a combination of conceptual models and HEC-RAS 5.0.5, this analysis leads to the following conclusions:

a) When subsidence changes the bed slope of a channel, changes in sediment transport can be expected. As shown in Figure 24 the sediment transport rates are higher on the upstream side of the subsidence induced sag because the slopes have increased, and sediment transport rates decrease in the decreasing limb where channel slopes have decreased. When the slope increased from 0.00019 m/m to 0.00025 m/m at Sta 300+00 in the 10 cms/m conceptual models the sediment transport rates increased from 129.9 metric tons/day/meter to 161 metric tons/day/meter. At Sta 100+00 a reduction in slope from 0.00042 m/m to 0.00027 m/m, attributed to subsidence produces a sediment transport rate reduction of approximately 125 metric tons/day/meter, from 251 metric tons/day/meter to 126 metric tons/day/meter.

b) Results from the Subsidence HEC-RAS model show negative cumulative mass bed changes on the upstream side of the subsidence induced sag where channel slopes

are increasing with values that are up to 11,500 tons more negative than the No Subsidence run which correlates to channel erosion of up to almost 2 feet. The section of the Bypass System that runs through the epicenter of the subsidence has up to 31,700 tons more cumulative mass bed change than in the No Subsidence run, indicating deposition, with values up to 2.1 more feet of deposition. The downstream portion of the Bypass System, from 128+00 to the end shows very similar cumulative mass bed changes for both the No Subsidence and Subsidence models but that up to 2.9 feet more deposition is predicted in the Subsidence model when compared to the No Subsidence model.

Subsidence in the San Joaquin River valley is an ongoing issue. Land subsidence will continue to be an issue as long as groundwater pumping continues and rivers and bypasses are used to divert water. This study used a complicated modeling technique to analyze how subsidence changes sediment transport to understand the subsidence induced effects on sediment transport yielding valuable results to aid water managers in the San Joaquin River valley and other regions experiencing subsidence.

Susan Cundiff, P.E., CFM

8. References

Allen, A. S. (1969). Geologic Settings of Subsidence. *Reviews in Engineering Geology, 2*, 305-342.

Begin, Z., Meyer, D., & Schumm, S. (1981). Development of longintudinal profiles in response to base-level lowering. *Earth Surfaces Processes and Landforms, 6*, 49-68.

Begin, Z., Meyer, D., & Schumm, S. (1981). Development of longitudinal profiles in response to base-level lowering. *Earth Surfaces Processes and Landforms, 6*, 49-68.

Brookes, A. (1988). *Channelized Rivers: Perspectives for Enviorimental Management.* Chichester: Wiley and Sons.

Bull, W., & Miller, E. (1975). Land Settlement due to groundwater withdrawal in the Los Banos-Kettlement City area, California. Part 1: Changes in the hydrologic environment due to subsidence. *U.S. Geological Survey Professional Paper 437-E*, pp. E1-E71.

Cundiff, S. (2017). *CIVE 717: Computer Problem.* Fort Collins, Colorado: Prepared for Colorado State University's CIVE 717, River Mechanics.

Dahl, T. A., Heath, R. E., Gibson, S. A., & Nygaard, C. J. (2018). *HEC-RAS Unsteady Flow and Sediment Model of the Mississippi River: Tarbert Landing to the Gulf.* Vicksburg, MS: U.S. Army Corphs of Engineers, Mississippi Valley Division.

DWR. (1969). *Lower San Joaquin River Flood Control Project, Final Design Report.* Division of Design and Construction.

DWR. (2018). *Draft Evaluation of the Effects of Subsidence and Sediment Transport on Channel Capacity in the Eastside Bypass and REach 4A of the San Joquin River.* Fresno, California: California Department of Water Resources.

Engelund, F., & Hansen, E. (1967). *A monograph on Sediment Transport in Alluvial Streams.* Copenhagen: Teknisk Forlag.

Farr, T., Jones, C., & Liu, Z. (2015). *Progress Report: Subsidence in the Central Valley, California.* Jet Propulsion Laboratory. California Institute of Technology.

Galloway, D., Jones, D., & Ingebritsen, S. (1999). *Land subsidence in the United States, Circular 1182.* U.S. Geological Survey.

Huang, & Greimann. (2008). *DRAFT Sediment Transport and channel morphology model in the San Joaquin River from Friant Dam to Mendota Dam.* Bureau of Reclamation, Denver Technical Services Center.

Julien, P. Y. (2010). *Erosion and Sedimentation, 2nd Edition.* Cambridge: Cambridge University Press.

Lofgren, B. (1960). Near-surface land subsidence in western San Joaquin Valley, California. *Journal of Geophysical Research, 65*(3), 1053-1062.

McBain & Thrush, Inc. (eds.). (2002). *San Joaquin River Restoration Study Bacground Report.* prepared for Friant Water Users Authority, Lindsay, CA and Natural Resources Defense Council, San Francisco, CA.

Mussetter Engineering Inc. (1996). *Evaluation of Potential Effects of Subsidence on The Genesee River and Tributaries.* Fort Collins: Mussetter Engineering Inc. submitted to Akzo Nobel Salt Inc.

Mussetter Engineering Inc. (2002). *Hydraulic and Sediment Continuity Modeling of the San Joaquin River from Friant Dam to Mendota Dam, California.* Fresno: Prepared by Mussetter Engineering, Inc. for the Bureau of Reclamation.

Ouchi, S. (1985). Response of alluvial rivers to slow active tectonic movement. *Geological Society of America Bulletin*, 504-515.

Poland, J. (1984). Guidebook to studies of land subsidence due to ground-water withdrawal. In W. G. 8.4 (Ed.). Paris: Prepared for the International Hydrological Programme.

RBF. (2013). *CVFED Model Documentation Report.* Technical Memorandum Upper San Joaquin River HEC-RAS Model Dcoumentation Task Order Number 24 (ST10).

Reclamation. (2012). *San Joaquin River Restoration Daily Flow Model (SJRRW) Documentation for the Reach 4B Study. Tecnical Report No. 86-68210-2012-04.* U.S. Bureau of Reclamation.

San Joaquin River Restoration Program. (2008). *Draft Bed Sediment Report, Sediment Sampling.*

Schumm, S., Dumont, J., & Holbrook, J. (2000). *Active Tectonics and Alluvial Rivers.* Cambridge University Press.

Susan Cundiff, P.E., CFM

Schumm, S., Harvey, M., & Watson, C. (1984). *Incised Channels Morpohology, Dynamics and Control.* Littleton, Colorado: Water Resources Publications.

SJRRP. (2014). *Subsidence Monitoring 2011-2013, Tehnical Memorandum.* Retrieved from www.restoresjr.net

SJRRP. (2015). *U.S. Bureau of Reclamation Static GPS Survey for Subsidence Monitoring.* Retrieved from www.restoresjr.net

Straub, K., Paola, C., Kim, W., & Sheets, B. (2013). Experimental Investigation of Sediment-Dominated vs. Tectonics-Dominated Sediment Transport Systems in Subsiding Basins. *Journal of Sedimentrary Research, 83*, 1162-1180.

Swanson, A. (1998). Land Subsidence in the San Joaquin Valley, Updated to 1995. In J. Borchers, *Land subsidence case studies and current research: Proceedings of the Dr. Joseph f. Poland Symposium on Land Subsidence* (pp. 75-79). Association of Engineering Geologists Special Publication No. 8.

Tetra Tech Inc. . (2010). *Sediment-transport Continuity Analysis for Existing and Proposed Levee Setbacks in Reaches 2A and 2B of the San Joaquin River. Draft Technical Memorandum.* Fresno, California: Prepared for the California Department of Water Resources.

Tetra Tech Inc. . (2015a). *Sediment-continuity Analysis of the Chowchilla and Eastside Bypasses between the CCBP Control Structure and Mariposa Bypass Draft Technical Memorandum.* Fresno, California: Prepared for the California Dept. of Water Resources.

Tetra Tech Inc. (2015b). *Draft Mobile-boundary Sediment-transport Analysis of the Chowchila and Eastside Bypasses between the CCBP Control Structure and Mariposa Bypass Draft Technical Memorandum.* Fresno, California: Prepared for the California Department of Water Resources.

Tetra Tech Inc. (2015c). *Draft San Joaquin River In-channel Capacity Analysis.* Fresno, California: Prepared for the California Department of Water Resources.

Tetra Tech Inc. (2015d). *Reaches 3, 4A and Middle Eastside Bypass (MESB) Subsidence and Capacity Study.* Fort Collins.

U.S. Army Corps of Engineers. (1993). *HEC-6 Scour and Deposition in Rivers and Reservoirs User's Manual.* Davis, California: Hydrologic Engineering Center.

U.S. Army Corps of Engineers. (1998). *SAM Hydraulic Design Package for Channels User's Manual.* Vicksburg, MS: Waterways Experiement Station.

U.S. Army Corps of Engineers. (2003). *SamWin Hydraulic Design Package.* Engineer Research Development Center, licensed to Mussetter Engineering, Inc. License Number 10.03019, February 16, 2006.

U.S. Army Corps of Engineers. (2016). *HEC-RAS Hydraulic Reference Manual Version 5.0.3.* Davis, California.

U.S. Army Corps of Engineers. (2018). *HEC-RAS Hydraulic Reference Manual Version 5.0.5.* Davis, California.